2014

Probing New Physics Through Third Generation Leptons

Preet Sharma
University of Mississippi

PROBING NEW PHYSICS WITH THIRD GENERATION LEPTONS

A dissertation
presented in partial fulfillment of requirements
for the degree of Doctor of Philosophy
in the Department of Physics and Astronomy
University of Mississippi

by

Preet Sharma

December 2014

ABSTRACT

This dissertation is a study of beyond standard model physics or new physics. The third generation charged lepton -the τ -is an excellent probe of new physics (NP) because of it being the heaviest lepton. As the heaviest lepton, it has the largest coupling (among the leptons) to the Higgs boson in the Standard Model (SM).

New physics contributions to the tau-neutrino nucleon scattering were considered. Charged Higgs and W' effects to the deep inelastic scattering $\nu_\tau(\bar{\nu}_\tau) + N \to \tau^-(\tau^+) + X$ in the neutrino-nucleon interactions has been studied. The neutrino detection process at neutrino oscillation experiments modify the measured atmospheric and reactor mixing angles θ_{23} and θ_{13}, respectively. A significant deviation from the standard model was observed in terms of the neutrino mixing angles.

The semileptonic decays of B meson to the τ lepton is mediated by a W boson in the SM. In many models of NP this decay gets contributions from additional states like new vector bosons, leptoquarks or new scalar particles. These new states affect the semileptonic $b \to c$ and $b \to u$ transitions and gave rise to new physics beyond the standard model. We have presented the angular distribution for $\bar{B} \to D^{*+}\tau^-\bar{\nu_\tau}$ with the most general new physics structure including tensor operators. We have then discussed the effects of the tensor operators on various observables that can be constructed out of the angular distribution. Our focus was on the azimuthal observables which include the important CP violating triple product asymmetries. We found that these azimuthal asymmetries, have different sensitivities to different new physics structures and hence they are powerful probes of the nature of the NP.

DEDICATION

To my wife Dittika and my daughter Preettika.

ACKNOWLEDGEMENTS

I would like to thank my advisor Dr. Alakabha Datta for supporting me during this time. He has given me freedom to pursue different problems while giving valuable advice to keep me on track. Not only academically, he has helped me every way possible during this time. I am truly lucky to have met such a wonderful person and I always appreciate his support. I wish that some day I could be as motivated and as efficient like him.I am also very grateful to Dr. Murugeswaran Duraisamy for his encouragements, scientific advice and suggestions. I also like to thank my Ph.D. committee members Dr. Don Summers, Dr. Lucien Cremaldi, Dr. Luca Bombelli and Dr. Micah B. Milinovich for support and effort for reviewing my work.

I would like to thank the Department of Physics and Astronomy, University of Mississippi for giving me the opportunity to teach Astronomy. I cannot be thankful enough for what I have learnt during this time.

I would also like to thank my colleagues Dr. Ahmed Rashed, Shanmuka Shivshankara, Hongkai Liu and Wanwei Wu for the collective efforts.

TABLE OF CONTENTS

LIST OF FIGURES

CHAPTER 1
MOTIVATION

1.1 Introduction

This dissertation is a study of some aspects of physics involved with the third generation leptons, namely, the τ and the ν_τ. The third generation charged lepton is an excellent probe of new physics (NP) because of it being the heaviest lepton. As the heaviest lepton, it has the largest coupling (among the leptons) to the Higgs boson in the Standard Model (SM). The τ lepton interacts only with the electroweak force and so does not suffer from the SM Quantum Chromodynamics(QCD) higher order corrections which are difficult to calculate. Hence NP effects in the τ sector can be easily isolated from the SM background. Also, the constraints on new physics involving the third generation leptons, the τ and ν_τ, are somewhat weaker, allowing for larger new physics effects. Experimentally, the τ production and decay are well separated in time allowing for measurements of the τ polarization and parity of the decaying objects which can be used to probe NP.

There are scenarios in which decays involving the τ leptons are very important probes of NP. Neutrino-Nucleon scattering is one of the cases in which a tau-neutrino scatters off a nucleon resulting in a tau lepton as one of the products. Here one can look at the different types of scattering such as the Quasi-Elastic scattering, Resonance scattering and Deep-inelastic scattering. Another sector in which the tau lepton plays an important role in NP search is CP violation. Tau is the only lepton that can decay to hadrons, which can provide an opportunity to observe non-SM type CP violation. The decays $B \to \tau\nu_\tau$, $B \to D^{(*)}\tau\nu_\tau$ and $B \to K^{(*)}\tau\tau$ are other examples where it may be possible to find new physics (NP) involving the third generation leptons. In fact in some of these decays, $B \to \tau\nu_\tau$, $B \to D^{(*)}\tau\nu_\tau$, there are disagreement between the SM predictions and

experimental results.

1.1.1 ν_τ scattering

An important place to consider nonstandard interactions (NSI) is ν_τ scattering. One such example is the $\nu_\tau + N \to \tau^- + X$ reaction, where $N = p, n$ is a nucleon and X is a possible final state. In the Standard Model the above interaction is mediated by a W boson. If we consider NSI by using a W' gauge boson or a charged Higgs, then we may see some deviations from the SM results. These deviations from the SM will be the deviations in the SM results of the neutrino mixing angles. We have worked out the details of non-standard interactions in ν_τ scattering through the Quasi-elastic scattering, Δ-Resonance scattering and Deep-inelastic scattering. We have also worked out, in the above three processes, the effects of NSI on the polarization of the τ. This will be explained in more detail in one of the following sections.

1.1.2 τ CP violation

CP violation in the SM is restricted to the quark sector and is forbidden in lepton decays. Moreover, the SM explanation of CP violation does not fully account for the large discrepancy between matter and anti-matter in the present universe. However, extensions to the SM do permit CP violations in τ decay. Searching for CP-violating decays in the lepton sector may help identify the missing contribution to the matter-antimatter asymmetry in the Universe. Among the three charged leptons, CP violation with the τ lepton has not been extensively studied . Hence searches for CP violation in τ decays are interesting probes for new physics scenarios. The result for one such decay has been discussed in Bigi and Sanda Ref. (*I.I.Bigi and A.I.Sanda*, 2005) predicted that, in the SM, the decay of the τ lepton to final states containing a ${K_S}^0$ will exhibit a nonzero decay rate asymmetry due to CP violation in $K^0 - \bar{K}^0$ mixing. The decay rate asymmetry, defined as

$$A = \frac{\Gamma(\tau^+ \to \pi^+ {K_S}^0 \bar{\nu}_\tau) - \Gamma(\tau^- \to \pi^- {K_S}^0 \nu_\tau)}{\Gamma(\tau^+ \to \pi^+ {K_S}^0 \bar{\nu}_\tau) + \Gamma(\tau^- \to \pi^- {K_S}^0 \nu_\tau)} \tag{1.1}$$

was predicted to be $(0.33 \pm 0.01)\%$, and a significant deviation from this value would be evidence of NP. As pointed out by Grossman and Nir Ref. (*Y.Grossman and Y.Nir*, 2002), the SM prediction for A has to be corrected for a factor due to the ${K^0}_S - \bar{K}^0_L$ interference. The corrected value for A is $(0.36 \pm 0.01)\%$. The decay-rate asymmetry has been measured to be $A = (-0.36 \pm 0.23 \pm 0.11)\%$ which is 2.8 standard deviations from the SM prediction of $(0.36 \pm 0.01)\%$. This could possibly be a hint of new physics beyond the SM.

1.1.3 $B \to \tau\nu$

B physics plays an important role in testing the Standard Model (SM). The decay $B \to \tau\nu$ is one such decay which may be giving hints of new physics because of the disagreement between the SM prediction and the experimental results. Measurements of branching ratios of $B \to \tau\nu$ and $B \to D^{(*)}\tau\nu$ probe the possible impact of beyond SM physics in the leptonic and semileptonic B-decays. Within the SM, these decay modes are important since they are used in obtaining precise values of $|V_{ub}|$ and $|V_{cb}|$ together with the relevant hadronic decay constants or form factors. For example, due to the large mass of the τ, semileptonic decays are sensitive to additional form factors, which are unimportant in the corresponding B decays with light leptons in the final state. Also, these tauonic decay modes represent sensitive tests of lepton flavor universality (LFU) in charged current interactions. The most recent world average of the leptonic $B \to \tau\nu$ branching fraction measurements, as reported by the Belle and BaBar Collaborations, is

$$Br(B \to \tau\nu) = (11.4 \pm 2.3) \times 10^{-5}. \tag{1.2}$$

This deviates from the SM prediction of

$$Br(B \to \tau\nu)_{SM} = (7.57^{+0.98}_{-0.61}) \times 10^{-5}. \tag{1.3}$$

The latest Belle result is

$$Br(B \to \tau\nu)_{SM} = (7.2^{+0.27}_{-0.25} \pm 0.11) \times 10^{-5}. \tag{1.4}$$

We see that the current world average of the experimental values still deviates from the SM prediction by 2.6σ. These results give a hint that NP effects may play a role in these decays.

1.1.4 $B \to D^* \tau^- \bar{\nu_\tau}$

The search for new physics (NP) beyond the Standard Model (SM) of particle physics is going on at the energy frontier in colliders such as the LHC and at the intensity frontier at high luminosity experiments. In the intensity frontier, the B factories, BaBar and Belle, have produced an enormous quantity of data and there is still a lot of data to be analyzed from both experiments. The LHCb and Belle II will continue the search for NP through precision measurements in the b quark system. There are a variety of ways in which NP in B decays can be observed Ref. (*A.Datta and D.Ghosh*, 2014; *A.Datta and P.J.O'Donnel*, 2005; *A.Datta*, 2006; *C.-W.Chiang and A.Szynkman*, 2010; *A.Datta and D.London*, 2004a; *S.Baek and D.London*, 2005; *A.Datta and R.Sinha*, 2005). In this NP search, the second and third generation quarks and leptons may be quite special because they are comparatively heavier and could be relatively more sensitive to NP. As an example, in certain versions of the two Higgs doublet models (2HDM) the couplings of the new Higgs bosons are proportional to the masses and so NP effects are more pronounced for the heavier generations. Moreover, the constraints on NP involving, specially the third generation leptons and quarks, are somewhat weaker allowing for larger NP effects Ref. (*A.Rashed and A.Datta*, 2013, 2012; *M.Duraisamy and A.Datta*, 2011; *A.Datta and M.Duraisamy*, 2010; *A.Datta and T.Huang*, 2000). This is explained in detail in chapter 4.

Recently we have been looking into the new physics in the decay of $\Lambda_b \to$ to Λ_c .

CHAPTER 2
Standard Model of Particle Physics

2.1 Standard Model

The visible Universe is composed of fermions and bosons and they are distinguished by their spin angular momentum. The fermions follow the Fermi-Dirac statistics and have half-integer spin. The bosons follow the Bose-Einstein statistics and possess integer spin. The four fundamental forces described by the Standard Model are the electromagnetic force, the weak force, the strong force and the gravitational force. Gravity is not included in the Standard Model because it is negligible due to the small masses of the elementary particles. The fermions are responsible for the matter of the Universe and the bosons are the mediators.

The fermions can be divided into two categories, namely 'leptons' and 'quarks'. The leptons are divided into three generations. The first generation consists of the electron (e) and the electron-neutrino (ν_e). The second generation consists of the muon (μ) and the muon-neutrino (ν_μ). The third generation consists of the tau (τ) and the tau-neutrino (ν_τ). The electron, muon and tau each have single unit electric charge, but their neutrinos are neutral electrically. The fermions experience the weak force and the charged fermions also experience the electromagnetic force. The carriers of the weak force are the Z and the W bosons, and the carrier of the electromagnetic force is the photon.

The quarks are of six types and they are up (u), down (d), strange (s), charm (c), bottom (b) and top (t). They have fractional charge. u, c, t have +2/3 charge and d, s, b have -1/3 charge. More details are given in Fig 2.1. Quarks are not found to exist individually. They are found in bound states like hadrons, baryons or mesons. The nucleons are made up of three quarks and the mesons are made up of quark-antiquark pairs. The force carriers of the quarks are the gluons.

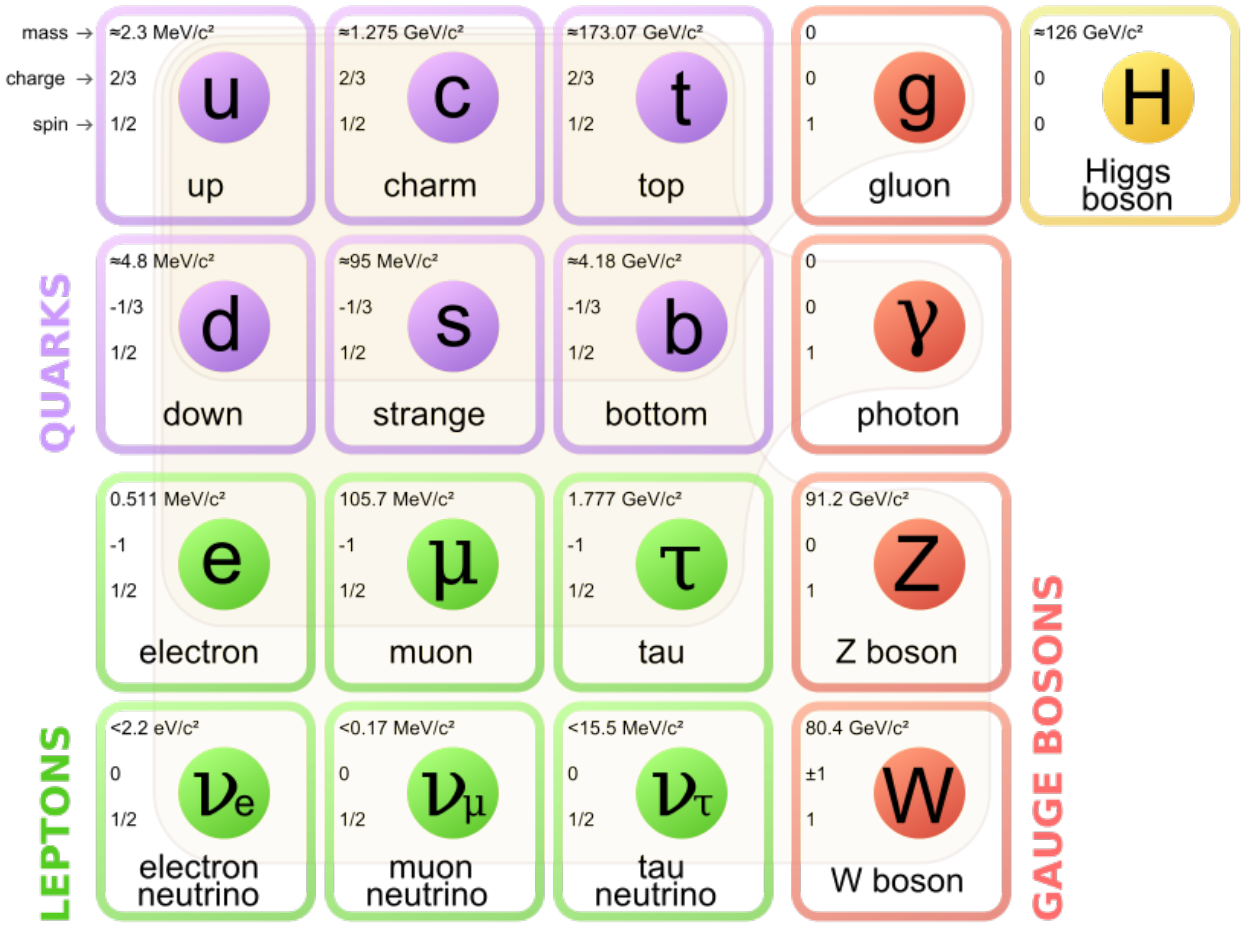
mass →
charge →
spin →
≈2.3 MeV/c²
2/3
1/2
u
up
≈1.275 GeV/c²
2/3
1/2
c
charm
≈173.07 GeV/c²
2/3
1/2
t
top
0
0
1
g
gluon
≈126 GeV/c²
0
0
H
Higgs boson
QUARKS
≈4.8 MeV/c²
-1/3
1/2
d
down
≈95 MeV/c²
-1/3
1/2
s
strange
≈4.18 GeV/c²
-1/3
1/2
b
bottom
0
0
1
γ
photon
0.511 MeV/c²
-1
1/2
e
electron
105.7 MeV/c²
-1
1/2
μ
muon
1.777 GeV/c²
-1
1/2
τ
tau
91.2 GeV/c²
0
1
Z
Z boson
LEPTONS
<2.2 eV/c²
0
1/2
νe
electron neutrino
<0.17 MeV/c²
0
1/2
νμ
muon neutrino
<15.5 MeV/c²
0
1/2
ντ
tau neutrino
80.4 GeV/c²
±1
1
W
W boson
GAUGE BOSONS

Figure 2.1:

2.2 The Electroweak Theory

The Electroweak theory is a unified description of the electromagnetic theory and the weak interaction. The electromagnetic force is described by the exchange of a photon and the weak theory is described by the exchange of W and Z bosons. It was first explained by Glashow, Weinberg and Salam, and it unifies the electromagnetic and the weak interactions.
The electroweak Langrangian can be written as

$$\mathcal{L}_{EW} = \mathcal{L}_g + \mathcal{L}_f + \mathcal{L}_h + \mathcal{L}_y \tag{2.1}$$

The kinetic energy term for the gauge boson is given by

$$\mathcal{L}_g = -\frac{1}{4}(A^a_{\mu\nu})^2 - \frac{1}{4}(B_{\mu\nu})^2 \tag{2.2}$$

where

$$X^a_{\mu\nu} = \partial_\mu X^a_\nu - \partial_\nu X^a_\mu + g f^{abc} X^b_\mu X^c_\nu \tag{2.3}$$

is known as the gauge boson field strength. The kinetic energy term for the fermions are

$$\mathcal{L}_f = \bar{E}_L(i\gamma_\mu D^\mu)E_L + \bar{e}_R(i\gamma_\mu D^\mu)e_R + \bar{Q}_L(i\gamma_\mu D^\mu)Q_L + \bar{d}_R(i\gamma_\mu D^\mu)d_R + \bar{u}_R(i\gamma_\mu D^\mu)u_R \tag{2.4}$$

where E_L are the left-handed lepton doublets, e_R are the right-handed leptons, Q_L are the left-handed quark doublets, d_R are the down-type right-handed quarks and u_R are the up-type right-handed quarks.

The Higgs term is

$$\mathcal{L}_h = |D_\mu\phi|^2 + \mu^2\phi^\dagger\phi - \lambda\phi^\dagger\phi^2 \tag{2.5}$$

This term contains the Higgs kinetic energy and the Higgs potential energy. For spontaneous symmetry breaking, the potential should have a minimum and it must be that $\mu^2 > 0$. The Yukawa interaction terms between the Higgs and the fermions are given as

$$\mathcal{L}_y = -Y_d \bar{Q}_L \cdot \phi d_R - Y_u \epsilon^{ab} \bar{Q}_{La} \cdot \phi^\dagger u_R - Y_e \bar{E}_L \cdot \phi e_R + h.c. \tag{2.6}$$

where Y_d, Y_e and Y_u are the Yukawa coupling constants and ϵ^{ab} is the totally antisymmetric tensor.

2.3 Beyond The Standard Model

The main motivation of this thesis is to look for beyond standard model physics or new physics. The best way to explain it is to describe it as quoted by Steven Weinberg:

It describes everything we see in the laboratory. Aside from leaving gravity out, it's a complete theory of what we see in nature. But it's not an entirely satisfactory theory, because it has a number of arbitrary elements. For example, there are a lot of numbers in this standard model that appear in the equations, and they just have to be put in to make the theory fit the observation. For example, the mass of the electron, the masses of the different quarks, the charge of the electron. If you ask, "Why are those numbers what they are? Why, for example, is the top quark, which is the heaviest known elementary particle, something like 300,000 times heavier than the electron?" The answer is, "We don't know. That's what fits experiment." That's not a very satisfactory picture.

CHAPTER 3
TAU NEUTRINO AS A PROBE OF NONSTANDARD INTERACTIONS

3.1 Introduction

Neutrino oscillation results have confirmed that neutrinos are massive and lepton flavors are mixed. This opens a window for searching physics beyond the standard model (SM). Beside the standard matter effects, the possibility of having nonstandard neutrino interactions (NSIs) is opened up. Nonstandard neutrino interactions with matter have been extensively discussed Ref. (*Wolfenstein*, 1978; *Mikheyev and Smirnov*, 1985; *M.C.Gonzalez-Garcia and Funchal*, 1999; *M.M.Guzzo and S.T.Petcov*, 1991; *S.Bergmann and H.Nunokaw*, 2000; *M.M.Guzzo and O.L.G.Peres*, 2001; *M.Guzzo and J.W.F.Valle*, 2002; *Y.Grossman*, 1995; *T.Ota and J.Sato*, 2002; *A.Friedland and C.Lunardini*, 2005; *N.Kitazawa and O.Yasuda*, 2006; *A.Friedland and C.Lunardini*, 2006; *M.Blennow and J.Skrotzki*, 2008; *A. Esteban-Pretel and Huber*, 2008; *M. C. Gonzalez-Garcia and Nir*, 2001; *A. M. Gago and Funchal*, 2001; *Huber and Valle*, 2001; *T. Ota and a. Yamashita*, 2002; *Campanelli and Romanino*, 2002; *M. Blennow and Winter*, 2007; *J. Kopp and Ota*, 2007; *J. Kopp and Sato*, 2008; *N. C. Ribeiro and Zukanovich-Funchal*, 2007; *N. C. Ribeiro and Minakata*, 2008; *J. Kopp and Winter*, 2008; *M. Malinsky and Zhang*, 2009; *A. M. Gago and Funchal*, 2010; *Palazzo and Valle*, 2009; *P. Coloma and Minakata*, 2011; *Super-Kamiokande*, 2011; *R. Adhikari and Roy*, 2012; *S. K. Agarwalla and Takeuchi*, 2012; *T. Ohlsson and Zhou*, 2013). General bounds on NSI are summarized in Ref. (*S. Davidson and Santamaria*, 2003; *DELPHI*, 2005; *C. Biggio and Fernandez-Martinez*, 2009). The NSI impact have been studied on solar neutrino Ref. (*Z. Berezhiani and Rossi*, 2002; *A. Friedland and Pena-Garay*, 2004; *O. G. Miranda and Valle*, 2006), atmospheric neutrinos Ref. (*S. Bergmann and Pierce*, 2000; *N. Fornengo and Valle*, 2002; *Gonzalez-Garcia and Maltoni*, 2004), reactor neutrinos Ref. (*F. J. Escrihuela and Valle*, 2009), and

neutrino-nucleus scattering Ref. (*J. Barranco and Rashba*, 2005, 2007).

At low energy, the most general effective NSI Lagrangian reads Ref. (*J. Kopp and Sato*, 2008), if we consider only lepton number conserving operators,

$$\mathcal{L}_{\rm NSI} = \mathcal{L}_{V\pm A} + \mathcal{L}_{S\pm P} + \mathcal{L}_{T}, \tag{3.1}$$

where the different terms are classified according to their Lorentz structure in the following way:

$$\begin{aligned}
\mathcal{L}_{V\pm A} &= \frac{G_F}{\sqrt{2}} \sum_{f,f'} \varepsilon_{\alpha\beta}^{f,f',V\pm A} \left[\bar{\nu}_\beta \gamma^\rho (1-\gamma^5) \ell_\alpha\right] \left[\bar{f}' \gamma_\rho (1 \pm \gamma^5) f\right] \\
&+ \frac{G_F}{\sqrt{2}} \sum_{f} \varepsilon_{\alpha\beta}^{f,V\pm A} \left[\bar{\nu}_\alpha \gamma^\rho (1-\gamma^5) \nu_\beta\right] \left[\bar{f} \gamma_\rho (1 \pm \gamma^5) f\right] + \text{h.c.}, \\
\mathcal{L}_{S\pm P} &= \frac{G_F}{\sqrt{2}} \sum_{f,f'} \varepsilon_{\alpha\beta}^{f,f',S\pm P} \left[\bar{\nu}_\beta (1+\gamma^5) \ell_\alpha\right] \left[\bar{f}' (1 \pm \gamma^5) f\right] + \text{h.c.}, \\
\mathcal{L}_{T} &= \frac{G_F}{\sqrt{2}} \sum_{f,f'} \varepsilon_{\alpha\beta}^{f,f',T} \left[\bar{\nu}_\beta \sigma^{\rho\tau} \ell_\alpha\right] \left[\bar{f}' \sigma_{\rho\tau} f\right] + \text{h.c.},
\end{aligned} \tag{3.2}$$

where G_F is the Fermi constant, ν_α is the neutrino field of flavor α, ℓ_α is the corresponding charged lepton field, and f, f' are the components of an arbitrary weak doublet. The dimensionless NSI parameters ε's represent the strength of the nonstandard interactions relative to G_F and we consider only left-handed neutrinos. This constraint on the neutrino chirality forbids $\nu\nu f f$ terms in $\mathcal{L}_{S\pm P}$ and $\mathcal{L}_T$. If the nonstandard interactions are supposed to be mediated by a new state with a mass of order $M_{\rm NSI}$, the effective vertices in Eq. (3.2) will be suppressed by $1/M_{\rm NSI}^2$ in the same way as the standard weak interactions are suppressed by $1/M_{\rm W}^2$. Therefore we expect that

$$|\varepsilon| \sim \frac{M_{\rm W}^2}{M_{\rm NSI}^2}. \tag{3.3}$$

In this work we considered the charged Higgs and W' gauge boson contributions to neutrino-nucleon scattering. Such new states arise in many extensions of the standard model and the phenomenology of these states have been widely studied. In this paper we have focussed on the

Δ-resonance production (Δ-RES) and deep inelastic scattering (DIS) in the interactions $\nu_\tau + N \rightarrow \tau^- + X$ and $\bar{\nu}_\tau + N \rightarrow \tau^+ + X$ where $N = p, n$ is a nucleon and X is a possible final state. In the Δ-RES production we have discussed the processes with $N = n, p$ and $X = \Delta^+, \Delta^0$, respectively. In the neutrino oscillation experiments, the neutrino-nucleus interaction in the detection process is assumed to be SM-like. Therefore, the extracted neutrino mixing angles, using the SM cross section, will have errors if there are new physics (NP) effects in the neutrino-nucleus amplitude. The NP effects modify the standard model cross section for $\nu_\tau + N \rightarrow \tau^- + X$ and thus impact the extraction of the atmospheric neutrino mixing angle θ_{23} in ν_τ appearance experiments. If high-energy Long Base Line (LBL) experiments (or atmospheric neutrino experiments scanning in the multi-GeV neutrino energy range) could measure θ_{13} via ν_τ appearance then the NP effects in $\nu_\tau + N \rightarrow \tau^- + X$ and $\bar{\nu}_\tau + N \rightarrow \tau^+ + X$ would impact the θ_{13} measurement and a mismatch between this measurement and that performed at the reactors could be a hint of a NSI in the former. The deviation of the actual mixing angle from the measured one, assuming the standard model cross section, have been studied including form factor effects in the Δ-RES case.

In this work, we made the important assumption that NP effects only arise in the coupling between the new particles and the third generation leptons, neglecting possible (subleasing) NSI effects with the first two generations. With the above assumption we can neglect NSI effects at productions since at production we have neutrino interactions involving the first and second generation leptons, only. Furthermore, the effect on ν_τ propagation can come only from neutral current interaction. Multi Higgs models and models with W' also generally contain neutral current interactions but the connection between the charged current and neutral current interactions is model dependent. We only considered the charged current interactions, and the addition of neutral current interactions would add another model dependent parameter in our calculation. We hope to include in future work also neutral current interactions.

This pattern of NP is common in many NP models Ref. (*A.Friedland and C.Lunardini*, 2006; *A. Esteban-Pretel and Huber*, 2008). For instance, in multi Higgs doublet models NP effects for the third generation quarks and leptons are enhanced because of their larger masses. For the W'

model we are assuming a W' with non-universal coupling to the generations. This is not an unusual scenario and would avoid constraints from W' searches at colliders that look at the decays to W' to first and second generation leptons. The reaction $\nu_\tau + N \to \tau^- + X$ is relevant to experiments like Super-Kamiokande (Super-K) Ref. (*Super-Kamiokande*, 2012) and OPERA that seek to measure $\nu_\mu \to \nu_\tau$ oscillation by the observation of the τ lepton. The DONuT experiment Ref. (*et al. (DONuT Collaboration)*, 2008) Ref. (*Kodama et al.*, 2001; *et al. (OPERA Collaborarion)*, 2010) measured the charged-current (CC) interaction cross section of the tau neutrino. A neutrino factory would be a prolic source of tau neutrinos via oscillation Ref. (*Neuffer*, 1981; *Alsharoa et al.*, 2003). The central-value results show deviation from the standard model predictions by about 40% but with large experimental errors; thus, the measurements are consistent with the standard model predictions. In this work we considered NP effects within a neutrino energy range higher than the threshold energy for the τ production where the Δ-RES and DIS contributions are dominant. Near threshold quasielastic scattering is important. The charged Higgs and W' contributions to the quasielastic (QE) scattering $\nu_\tau + n \to \tau^- + p$ and $\bar{\nu}_\tau + p \to \tau^+ + n$ were considered in an earlier paper Ref. (*A. Rashed and Datta*).

The hadronic transition in the charged-current (CC) interactions $\nu_\tau + N \to \tau^- + X$ and $\bar{\nu}_\tau + N \to \tau^+ + X$ at the partonic level is described by $(u, d) \to q$, where q is a quark. In the Δ-RES case $q = u, d$, while in the DIS the main contributions are obtained when $q = u, d$ because of the CKM factors. This means that the effective operator of these interactions mainly has the structure $\mathcal{O}_{NP} = \bar{u}\Gamma_i d\bar{\tau}\Gamma_j$, where $\Gamma_{i,j}$ are some Dirac structures. Therefore, we can constrain the NP parameters in this work using the constraints that have been discussed in the earlier paper Ref. (*A. Rashed and Datta*) through the τ decay modes $\tau^- \to \pi^-\nu_\tau$ and $\tau^- \to \rho^-\nu_\tau$. These decay channels have operator structures similar to the one in the above CC interactions.

In Ref. (*A. Rashed and Datta*), we presented a model independent analysis of the NP contributions to the deviations of the mixing angles θ_{23} and θ_{13}. In the case of θ_{23}, the relationship between the ratio of the NP contribution to the SM cross section $r_{23} = \sigma_{NP}(\nu_\tau)/\sigma_{SM}(\nu_\tau)$ and the deviation δ_{23} of the mixing angle was obtained in a model independent form as

$$r_{23} \;=\; \Big[\frac{\sin 2(\theta_{23})_{SM}}{\sin 2(\theta_{23})}\Big]^2 - 1\,. \tag{3.4}$$

Here, $\theta_{23} = (\theta_{23})_{SM} + \delta_{23}$ is the actual atmospheric mixing angle, whereas $(\theta_{23})_{SM}$ is the extracted mixing angle assuming the SM ν_τ scattering cross section and δ_{23} is the deviation . From figure (1) in Ref. (*A. Rashed and Datta*), one can see that $\delta_{23} \sim -5^\circ$ requires $r_{23} \sim 5\%$. Similarly for θ_{13} determination, the relationship between $r_{13} = \sigma_{NP}(\bar{\nu}_\tau)/\sigma_{SM}(\bar{\nu}_\tau)$ and δ_{13} is given by

$$r_{13} \;=\; \Big[\frac{\sin 2(\theta_{13})_{SM}}{\sin 2(\theta_{13})}\Big]^2 - 1\,, \tag{3.5}$$

with $\theta_{13} = (\theta_{13})_{SM} + \delta_{13}$. In this case, because of the relative smallness of θ_{13} one finds that a larger NP effect is required to produce the deviation. As an example, $\delta_{13} \sim -1^\circ$ requires $r_{13} \sim 25\%$.

A possible concern was that the NP effects can be washed out after including the neutrino flux and integrating over the possible values of the incoming neutrino energy. It was shown that this is not the case by by considering examples of the W' and charged Higgs contributions to δ_{23} using the atmospheric neutrino flux at the Super-Kamiokande experiment. The results show that the values and the pattern of the mixing angle deviation δ_{23} has no significant change due to considering the neutrino flux.

We studied, also, the NP effect on the spin polarization of the produced τ lepton. The produced τ decays to several particles including ν_τ and tracing back the τ decay particle distributions indicates the appearance of τ. Because the τ decay distributions depend significantly on its spin polarization, the polarization information is essential to identify the τ production signal. Hence it is important to know how NP affects the τ polarization.

3.2 Kinematics and formalism

In the interactions $\nu_\tau(\bar{\nu}_\tau) + N \rightarrow \tau^-(\tau^+) + X$, we define the four-momenta of incoming neutrino (k), target nucleon (p) and produced τ lepton (k') in the laboratory frame. The hadronic invariant mass

$$W^2 = (p+q)^2, \tag{3.6}$$

where $q = k - k'$ is the four-momentum transfer, is defined in the allowed physical region

$$M \leq W \leq \sqrt{s} - m_\tau, \tag{3.7}$$

where $s = (k+p)^2$ is the center of mass energy and M is the average nucleon mass.

The three relevant subprocesses in the neutrino-nucleon interactions are classified according to the regions of the hadronic invariant mass W and the momentum transfer $q^2(= -Q^2)$ Ref. (*K. Hagiwara and Yokoya*, 2003). One can label QE (quasi-elastic scattering) when the hadronic invariant mass is equal to the nucleon mass $W = M$, RES (resonance production) when $M + m_\pi < W < W_{\rm cut}$, and IS (inelastic scattering) when $W_{\rm cut} < W < \sqrt{s} - m_\tau$. $W_{\rm cut}$, taken in the region 1.4 GeV$\sim$1.6 GeV, is an empirical boundary between RES and IS processes, to avoid double counting. The deep inelastic scattering DIS may be labeled within the IS region when $Q^2 \geq 1\ {\rm GeV}^2$, where the use of the parton model can be justified. In this work, we considered Δ-resonance state production and neglect all the other higher resonance states which gives small contributions Ref. (*Paschos and Yu*, 2002; *E. A. Paschos and Yu*, 2000). One can write

$$W^2 = M^2 + t + 2p \cdot q, \tag{3.8}$$

with $p \cdot q = M(E_\nu^{cm} - E_l^{cm})$ where the energy and momentum of the lepton and the neutrino in

the center of mass (cm) system are

$$\begin{aligned} E_{\nu}^{cm} &= \frac{(s-M^2)}{2\sqrt{s}}, \;\; p_l^{\rm cm} = \sqrt{(E_l^{cm})^2 - m_l^2}, \\ E_l^{cm} &= \frac{(s-M_\Delta^2+m_l^2)}{2\sqrt{s}}, \end{aligned} \tag{3.9}$$

with $(m_l,\ M,\ M_\Delta)$ being the masses of the charged lepton, nucleon, and the Δ state, respectively. In the lab frame, the charged lepton energy is given by

$$E_l = \frac{t + 2ME_\nu + M^2 - M_\Delta^2}{2M}. \tag{3.10}$$

The threshold neutrino energy to create the charged lepton partner in the Δ-RES case is given by

$$E_{\nu_l}^{\rm th} = \frac{(m_l + M_\Delta)^2 - M_n^2}{2M_n}, \tag{3.11}$$

which gives $E_{\nu_l}^{\rm th} = 4.35$ GeV in the case of tau neutrino production. Using the allowed range of the invariant mass in the resonance production, the allowed region of the momentum transfer $t \equiv -Q^2$ lies in the interval

$$(M+m_\pi)^2 - \left(M^2 + 2M(E_\nu^{\rm cm} - E_l^{\rm cm})\right) \leq t \leq W_{\rm cut}^2 - \left(M^2 + 2M(E_\nu^{\rm cm} - E_l^{\rm cm})\right). \tag{3.12}$$

3.3 Standard Model Cross Sections

In this section we considered the standard model cross sections for the DIS processes. In the following sections we have showed the contributions of the new states W' and charged Higgs to theses two processes. In Ref. Ref. (*A. Rashed and Datta*) the NP contributions to the QE process were studied.

3.3.1 Deep inelastic tau neutrino scattering

In this section, we present the standard model cross sections for the two deep inelastic scattering (DIS) processes which include ν_τ and $\bar{\nu}_\tau$,

$$\begin{aligned} \nu_\tau + N &\to \tau^- + X, \\ \bar{\nu}_\tau + N &\to \tau^+ + X. \end{aligned} \tag{3.13}$$

From Hagiwara model, see Ref. (*K. Hagiwara and Yokoya*, 2003) for details, the differential cross section can be parametrized as follows, for $Q^2 \ll m_W^2$,

$$\frac{d^2\sigma^{\nu_\tau(\bar{\nu}_\tau)}}{dxdy} = \left(\frac{G_F^2 V_{qq'}^2}{2\pi}\right) y \left(A\,W_1 + \frac{1}{M^2}B\,W_2 \pm \frac{1}{M^2}C\,W_3 + \frac{1}{M^2}D\,W_5\right)\delta(\xi - x), \tag{3.14}$$

where $p_q^\mu = \xi p^\mu$ is the four-momentum of the scattering quark and ξ is its momentum fraction. The coefficients A,B,C,D are defined as

$$\begin{aligned} A &= y\left(yx + \frac{{m_l}^2}{2E_\nu M}\right), \\ B &= \left(1 - \frac{{m_l}^2}{4{E_\nu}^2}\right) - \left(1 + \frac{Mx}{2E_\nu}\right) y, \\ C &= 2y\left(x\left(1 - \frac{y}{2}\right) - \frac{{m_l}^2}{4E_\nu M}\right), \\ D &= \frac{{m_l}^2}{E_\nu M}, \end{aligned} \tag{3.15}$$

where x is the Bjorken variable and y is the inelasticity and they are related by

$$x = \frac{Q^2}{2E_\nu M y}. \tag{3.16}$$

The functions $W_{1,2,3,5}$ are given in Ref. (*K. Hagiwara and Yokoya*, 2003).

3.4 Charged Higgs contribution

We have studied the contributions of the charged Higgs to the DIS interactions. The deviation of the actual mixing angles θ_{23} and θ_{13}, with NP contributions, from the measured ones, which assumes the SM cross section, have been discussed.

3.4.1 Deep inelastic tau neutrino scattering

We choose the couplings of charged Higgs interactions to the SM fermions to be given by the two Higgs doublet model of type II (2HDM II) Ref. (*Diaz*)

$$\mathcal{L} = \frac{g}{2\sqrt{2}}\left[V_{u_i d_j}\bar{u}_i(g_S^{u_i d_j} \pm g_P^{u_i d_j}\gamma^5)d_j + \bar{\nu}_i(g_S^{\nu_i l_j} \pm g_P^{\nu_i l_j}\gamma^5)l_j\right] H^{\pm}, \tag{3.17}$$

where u_i and d_j refer to up and down type quarks, and ν_i and l_j refer to neutrinos and the corresponding charged leptons. The other parameters are as follows: $g = e/\sin\theta_W$ is the SM weak coupling constant, $V_{u_i d_j}$ is the CKM matrix element, and $g_{S,P}$ are the scalar and pseudoscalar couplings of the charged Higgs to fermions. Here, in this work, we assume the couplings $g_{S,P}$ are real and given as

$$\begin{aligned} g_S^{u_i d_j} &= \left(\frac{m_{d_j}\tan\beta + m_{u_i}\cot\beta}{M_W}\right), \\ g_P^{u_i d_j} &= \left(\frac{m_{d_j}\tan\beta - m_{u_i}\cot\beta}{M_W}\right), \\ g_S^{\nu_i l_j} &= g_P^{\nu_i l_j} = \frac{m_{l_j}\tan\beta}{M_W}, \end{aligned} \tag{3.18}$$

where $\tan\beta$ is the ratio between the two vev's of the two Higgs doublets. From Eq. 3.17 we can construct the NSI parameters defined in Ref Ref. (*C. Biggio and Fernandez-Martinez*, 2009) as $\varepsilon_{\tau\tau}^{ud(L)} \equiv \frac{m_u m_\tau}{m_H^2}$ and $\varepsilon_{\tau\tau}^{ud(R)} \equiv \frac{m_d m_\tau \tan^2\beta}{m_H^2}$.

The charged Higgs contributions to the matrix elements of the interactions $\nu_\tau + N \to \tau^- + X$

and $\bar{\nu}_\tau + N \to \tau^+ + X$ are given by

$$
\begin{aligned}
M_H^{\nu_\tau} &= \left(\frac{G_F V_{qq'}}{\sqrt{2}}\right) X_H \, g_S^{\nu_\tau \tau} \, [\bar{u}_\tau(k')\,(1+\gamma_5) u_{\nu_\tau}(k)] \, \left[\bar{u}_{q'}(p'_{q'})(g_S^{qq'} + g_P^{qq'}\gamma_5)\, u_q(p_q)\right], \\
M_H^{\bar{\nu}_\tau} &= \left(\frac{G_F V_{qq'}}{\sqrt{2}}\right) X_H \, g_S^{\nu_\tau \tau} \, [\,\bar{v}_{\nu_\tau}(k)(1-\gamma_5) v_\tau(k')] \, \left[\bar{u}_{q'}(p'_{q'})(g_S^{qq'} - g_P^{qq'}\gamma_5)\, u_q(p_q)\right],
\end{aligned}
\tag{3.19}
$$

where $q, q' = (u_i, d_j)$ and the couplings $g_{S,P}^{qq'},\ g_S^{\nu_\tau \tau}$ are defined as in Eq. 3.18

The differential cross section is given by

$$
\begin{aligned}
\frac{d^2\sigma^{\nu_\tau(\bar{\nu}_\tau)}}{dxdy} &= \left(\frac{G_F^2 V_{qq'}^2}{2\pi}\right) X_H^2 \, (g_S^{v_l l})^2 \, y \, L_{\mu\nu}^{\nu_\tau(\bar{\nu}_\tau)} \, W^{\mu\nu} \, \delta(\xi - x) \\
&= \left(\frac{G_F^2 V_{qq'}^2 E_\nu \, M}{\pi}\right) X_H^2 \, (g_S^{v_l l})^2 \, \left[y\left(yx + \frac{{m_l}^2}{2E_\nu M}\right)\right] \\
&\quad \frac{1}{4} \, \left[(g_S^{qq'})^2 + (g_P^{qq'})^2\right] \, F_1 \, \delta(\xi - x),
\end{aligned}
\tag{3.20}
$$

where $X_H = M_W^2/M_H^2$ and the definitions of the 2HDM coupling constants are given in Eqs. 3.18.

There is no interference term of the SM and NP amplitudes. Thus, with the constraints on the NP parameters $(M_H,\ \tan\beta)$ Ref. (*A. Rashed and Datta*), the charged Higgs contributions relative to the SM $r_H^{23} = \sigma_H(\nu_\tau)/\sigma_{SM}(\nu_\tau)$ and $r_H^{13} = \sigma_H(\bar{\nu}_\tau)/\sigma_{SM}(\bar{\nu}_\tau)$ are small within the kinematical interval $W_{cut} < W < \sqrt{s} - m_\tau$ GeV with $W_{cut} = 1.4$ GeV. Thus, the deviations δ_{23} and δ_{13} of the mixing angles are negligibly small.

3.5 W' gauge boson contribution

We studied the contributions of the W' gauge boson to the DIS processes. The deviation of the mixing angles θ_{23} and θ_{13} were considered. The effective Lagrangian of W' interactions to the

SM fermions has the form

$$\mathcal{L} = \frac{g}{\sqrt{2}} V_{f'f} \bar{f}' \gamma^{\mu} (g_L^{f'f} P_L + g_R^{f'f} P_R) f W'_{\mu} + \ h.c., \tag{3.21}$$

where f' and f refer to the fermions and $g_{L,R}^{f'f}$ are the left and the right handed couplings of the W'. We will assume $g_{L,R}^{f'f}$ to be real. Constraints on the couplings in Eq. (3.21) come from the hadronic τ decay channels $\tau^- \to \pi^- \nu_\tau$ and $\tau^- \to \rho^- \nu_\tau$ discussed in Ref. (*A. Rashed and Datta*), which are consistent with the ones in Ref. (*C. Biggio and Fernandez-Martinez*, 2009). From Eq. (3.21), the NSI parameters $\varepsilon_{\tau\tau}^{ud(L,R)}$ defined in Ref. (*C. Biggio and Fernandez-Martinez*, 2009) are given as $\varepsilon_{\tau\tau}^{ud(L,R)} \equiv g_L^{\tau\nu} g_{(L,R)}^{ud} (\frac{M_W}{M_{W'}})^2$.

3.5.1 Deep inelastic tau neutrino scattering

The matrix elements are

$$\begin{aligned} M_{W'}^{\nu_\tau} &= \left(\frac{-iG_F V_{qq'} K_{W'}}{\sqrt{2}} \right) \left[\bar{u}_\tau(k') \gamma^\mu (1-\gamma_5) u_{\nu_\tau}(k) \right] \left[\bar{u}_{q'}(p'_{q'}) \, \gamma_\mu \left(\gamma_{W'}^{\rho} - \gamma_{W'}^{\kappa} \gamma_5 \right) u_q(p_q) \right], \\ M_{W'}^{\bar{\nu}_\tau} &= \left(\frac{-iG_F V_{qq'} K_{W'}}{\sqrt{2}} \right) \left[\bar{v}_{\nu_\tau}(k) \gamma^\mu (1-\gamma_5) v_\tau(k') \right] \left[\bar{u}_{q'}(p'_{q'}) \, \gamma_\mu \left(\gamma_{W'}^{\rho} - \gamma_{W'}^{\kappa} \gamma_5 \right) u_q(p_q) \right], \end{aligned} \tag{3.22}$$

where the definitions are

$$\begin{aligned} \gamma_{W'}^{\rho} &= X_{W'} g_L^{\nu_\tau \tau} (g_L^{qq'} + g_R^{qq'}), \\ \gamma_{W'}^{\kappa} &= X_{W'} g_L^{\nu_\tau \tau} (g_L^{qq'} - g_R^{qq'}), \\ X_{W'} &= \left(\frac{m_W^2}{m_{W'}^2} \right), \\ K_{W'} &= \left(1 + \frac{Q^2}{m_{W'}^2} \right)^{-1}. \end{aligned} \tag{3.23}$$

The total differential cross section has the same form as the SM one in Eq. (3.14), after setting $K^2_{W'} \sim 1$,

$$\frac{d^2\sigma^{\nu_\tau(\bar{\nu}_\tau)}_{SM+W'}}{dxdy} = \left(\frac{G_F^2 V_{qq'}^2}{2\pi}\right)\, y\left(A'\,W_1 + \frac{1}{M^2}B'\,W_2 \pm \frac{1}{M^2}C'\,W_3 + \frac{1}{M^2}D'\,W_5\right)\delta(\xi - x), \tag{3.24}$$

where A',B',C', and D' are defined as:

$$\begin{aligned} A' &= \frac{1}{2}A\left(|a'|^2 + |b'|^2\right), \\ B' &= \frac{1}{2}B\left(|a'|^2 + |b'|^2\right), \\ C' &= Re[a'b'^*]C, \\ D' &= \frac{1}{2}D\left(|a'|^2 + |b'|^2\right). \end{aligned} \tag{3.25}$$

with

$$\begin{aligned} a' &= 1 + \gamma^{\rho}_{W'}, \\ b' &= 1 + \gamma^{\kappa}_{W'}. \end{aligned} \tag{3.26}$$

The ratios of the W' contributions to the SM cross sections $r^{23}_{W'}$ and $r^{13}_{W'}$ and the deviations δ_{23} and δ_{13} are shown within the allowed kinematical range $M + m_\pi < W < 1.4$ GeV in Figs. (3.1, 3.2, 3.3, 3.4). The $r^{23}_{W'}$ and $r^{13}_{W'}$ values are mostly positive which, in turn, leads to δ_{23} and δ_{13} being mostly negative, respectively. As some examples, we find that $\delta_{23} \approx -14^\circ$ and $\delta_{13} \approx -1.5^\circ$ at $E_\nu = 17$ GeV, $M_{W'} = 200$ GeV, and $(g_L^{\tau\nu_\tau}, g_L^{ud}, g_R^{ud}) = (-0.94, -1.13, -0.85)$. In Fig. 3.5, the results show a negligible change to the δ_{23} values when considering the atmospheric neutrino flux Ref. (*M.Honda and S.Midorikawa*, 2011).

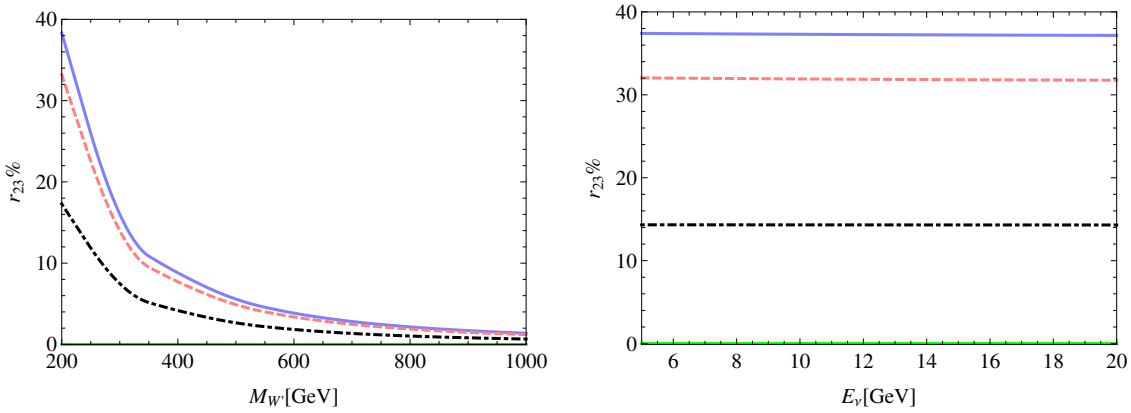

Figure 3.1: DIS (W'): The left (right) panel figures illustrate the variation of $r^{23}_{W'}\%$ with the W' mass $M_{W'}$ (E_ν) when both left and right-handed W' couplings are present. The lines show predictions for some representative values of the W' couplings $(g_L^{\tau\nu_\tau}, g_L^{ud}, g_R^{ud})$. The green line (solid, lower) corresponds to the SM prediction. The blue line (solid, upper) in the left figure corresponds to (-0.94 , -1.13 , -0.85) at $E_\nu = 17$ GeV, and the blue line (solid, upper) in the right figure corresponds to (1.23 , 0.84 , 0.61) at $M_{W'} = 200$ GeV.

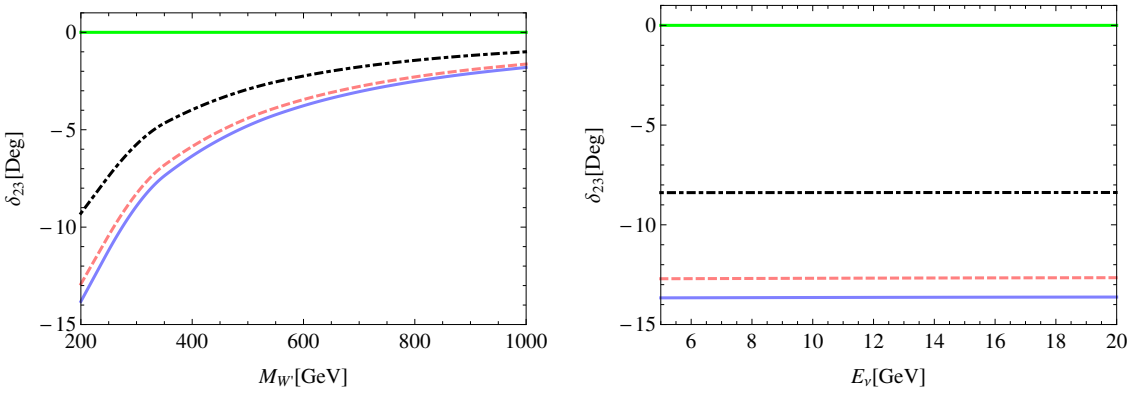

Figure 3.2: DIS (W'): The left (right) panel figures illustrate the deviation δ_{23} with the W' mass $M_{W'}$ (E_ν) when both left and right-handed W' couplings are present. The lines show predictions for some representative values of the W' couplings $(g_L^{\tau\nu_\tau}, g_L^{ud}, g_R^{ud})$. The green line (solid, upper) corresponds to the SM prediction. The blue line (solid, lower) in the left figure corresponds to (-0.94 , -1.13 , -0.85) at $E_\nu = 17$ GeV, and the blue line (solid, lower) in the right figure corresponds to (1.23 , 0.84 , 0.61) at $M_{W'} = 200$ GeV. Here, we use the best-fit value $\theta_{13} = 9.1^\circ$ Ref. (*D.V.Forero and J.W.F.Valle*).

3.6 Δ-Resonance production

Similar calculations were done considering the Δ-RES production in $\nu_\tau + n \to \tau^- + \Delta^+$ and $\bar{\nu}_\tau + p \to \tau^+ + \Delta^0$ in models with a W' gauge boson and a charged Higgs. The results are summarized in plots as shown below.

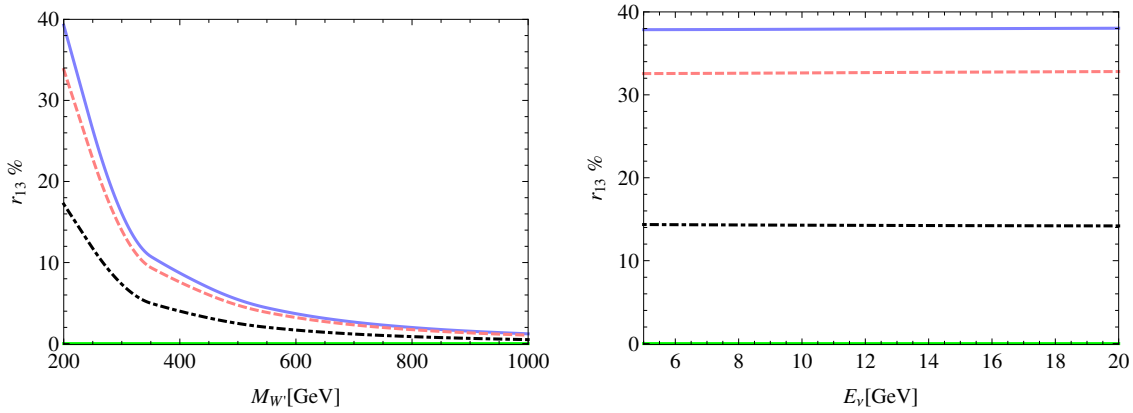

Figure 3.3: DIS (W'): The left (right) panel figures illustrate the variation of $r^{13}_{W'}\%$ with the W' mass $M_{W'}$ (E_ν) when both left and right-handed W' couplings are present. The lines show predictions for some representative values of the W' couplings $(g_L^{\tau\nu_\tau}, g_L^{ud}, g_R^{ud})$. The green line (solid, lower) corresponds to the SM prediction. The blue line (solid, upper) in the left figure corresponds to (-0.94 , -1.13 , -0.85) at $E_\nu = 17$ GeV, and the blue line (solid, upper) in the right figure corresponds to (1.23 , 0.84 , 0.61) at $M_{W'} = 200$ GeV.

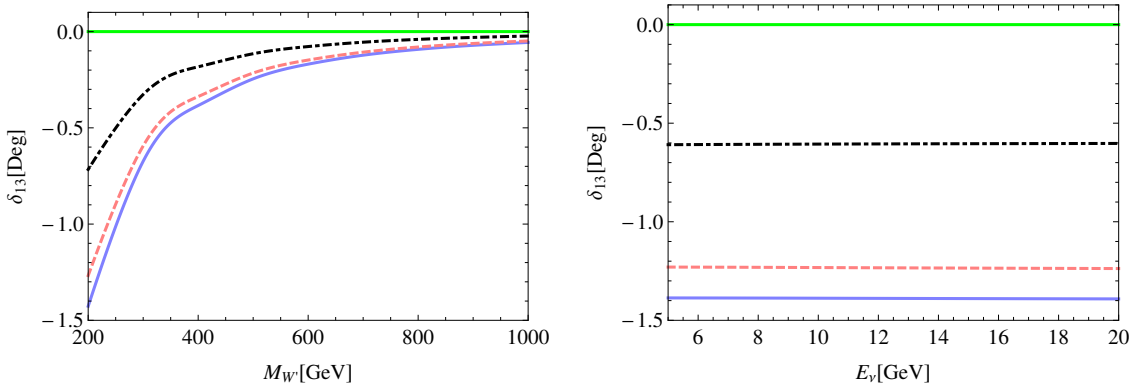

Figure 3.4: DIS (W'): The left (right) panel figures illustrate the deviation δ_{13} with the W' mass $M_{W'}$ (E_ν) when both left and right-handed W' couplings are present. The lines show predictions for some representative values of the W' couplings $(g_L^{\tau\nu_\tau}, g_L^{ud}, g_R^{ud})$. The green line (solid, upper) corresponds to the SM prediction. The blue line (solid, lower) in the left figure corresponds to (-0.94 , -1.13 , -0.85) at $E_\nu = 17$ GeV, and the blue line (solid, lower) in the right figure corresponds to (1.23 , 0.84 , 0.61) at $M_{W'} = 200$ GeV. Here, we use the best-fit value $\theta_{13} = 9.1^\circ$ Ref. (*D.V.Forero and J.W.F.Valle*).

3.7 Polarization of the produced $\tau^\pm$

In this section we studied the effects of NP on the polarization of the produced τ. The starting point was to construct the spin-density matrix $\rho_{\lambda,\lambda'}$, where λ and λ' are the helicity of the τ lepton. The spin-density matrix $\rho_{\lambda,\lambda'}$ is related to the spin dependent differential cross section as

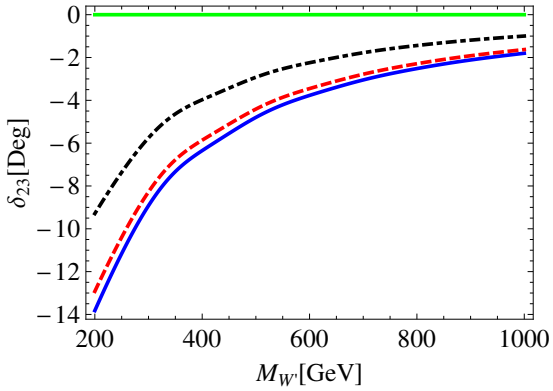

Figure 3.5: DIS (W'): The figure illustrates the deviation δ_{23} with the W' mass $M_{W'}$ when both left and right-handed W' couplings are present. The lines show predictions for some representative values of the W' couplings $(g_L^{\tau\nu_\tau}, g_L^{ud}, g_R^{ud})$. The green line (solid, upper) corresponds to the SM prediction. The blue line (solid, lower) corresponds to (-0.94 , -1.13 , -0.85). Here, we use the best-fit value $\theta_{23} = 42.8°$ Ref. (*M.C.Gonzalez-Garcia and J.Salvado*, 2010). We take into account the atmospheric neutrino flux for Kamioka where the Super-Kamiokande experiment locates Ref. (*M.Honda and S.Midorikawa*, 2011).

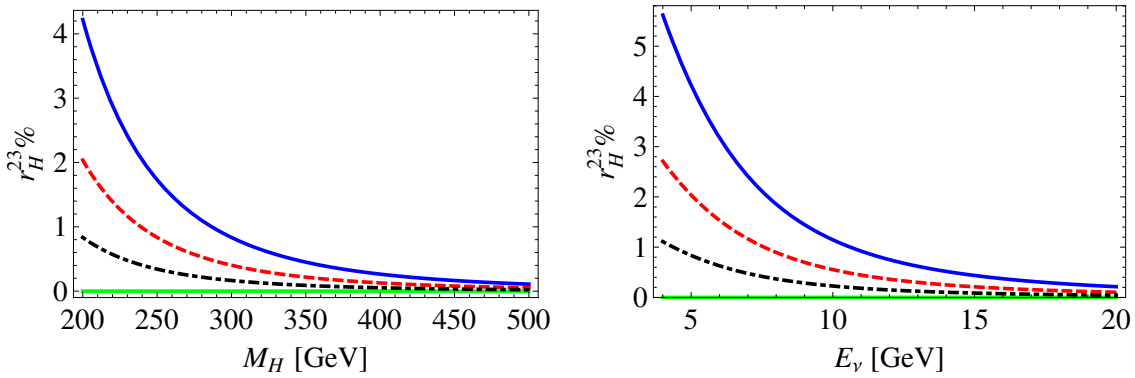

Figure 3.6: Resonance (H): The figures illustrate variation of $r_H^{23}\%$ with M_H (left) and E_ν (right). The green line corresponds to the SM prediction. The black (dotdashed), red (dashed), and blue (solid) lines correspond to $\tan\beta = 40, 50, 60$ at $E_\nu = 5$ GeV (left) and at $M_H = 200$ GeV (right).

$$\frac{d\sigma_{\lambda,\lambda'}}{dE_l d\cos\theta} = |\rho_{\lambda\lambda'}|^2 \frac{d\sigma_{total}}{dE_l d\cos\theta}, \tag{3.27}$$

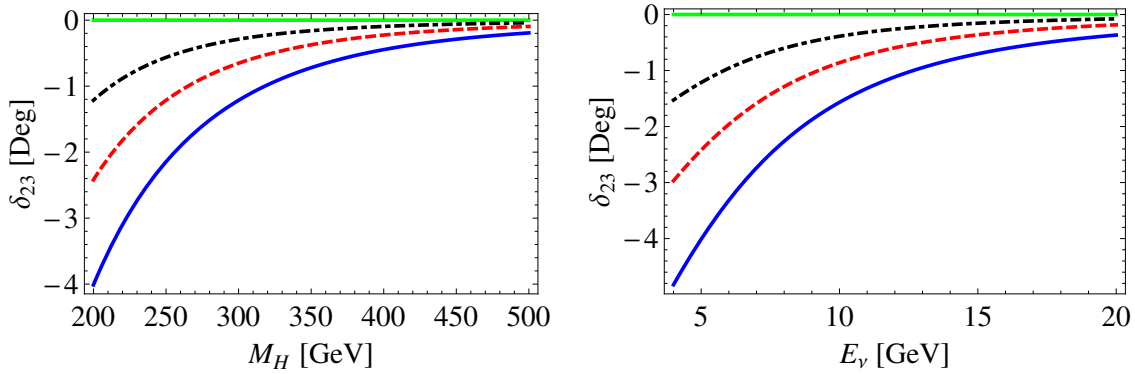

Figure 3.7: Resonance (H): The figures illustrate variation of δ_{23} with M_H (left) and E_ν (right). The green line corresponds to the SM prediction. The black (dotdashed), red (dashed), and blue (solid) lines correspond to $\tan\beta = 40, 50, 60$ at $E_\nu = 5$ GeV (left) and at $M_H = 200$ GeV (right). Here, we use the best-fit value $\theta_{23} = 42.8^\circ$ Ref. (*M.C.Gonzalez-Garcia and J.Salvado*, 2010).

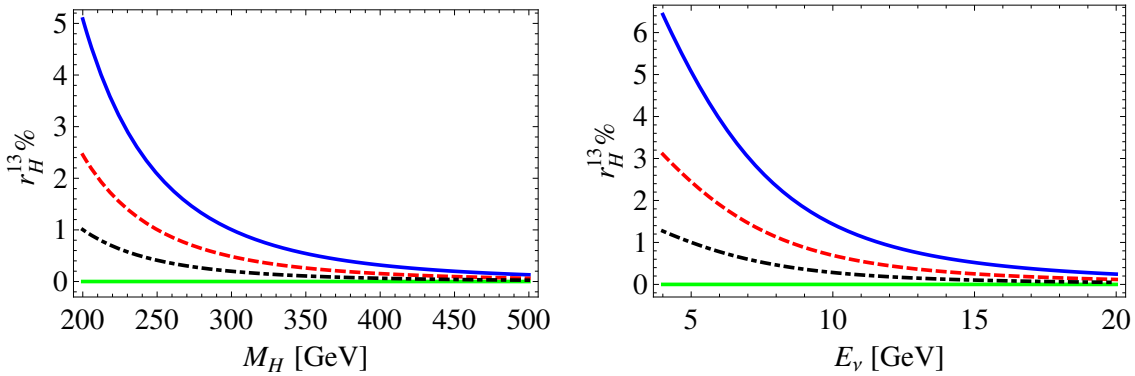

Figure 3.8: Resonance (H): The figures illustrate variation of $r_H^{13}\%$ with M_H (left) and E_ν (right). The green line corresponds to the SM prediction. The black (dotdashed), red (dashed), and blue (solid) lines correspond to $\tan\beta = 40, 50, 60$ at $E_\nu = 5$ GeV (left) and at $M_H = 200$ GeV (right).

where the total cross section $\sigma_{total} = \sigma_{\frac{1}{2}\frac{1}{2}} + \sigma_{-\frac{1}{2}-\frac{1}{2}}$. The spin-density matrix $\rho_{\lambda,\lambda'}$ is expressed in terms of the spin dependent matrix element $M_{\lambda,\lambda'} = L^{\mu\nu}_{\lambda,\lambda'} W_{\mu\nu}$ as

$$\rho_{\lambda,\lambda'} \;=\; \frac{\mathcal{M}_{\lambda,\lambda'}}{\sum_{\lambda=\pm\frac{1}{2}} \mathcal{M}_{\lambda,\lambda}}\,. \tag{3.28}$$

The most general form of the polarization density matrix ρ of a fermion is parametrized as

$$\rho \;=\; [\rho_{\lambda,\lambda'}] = \frac{1}{2}(I + \tau^a \cdot \vec{P}) = \frac{1}{2}\begin{pmatrix} 1+P_z & P_x - iP_y \\ P_x + iP_y & 1-P_z \end{pmatrix}, \tag{3.29}$$

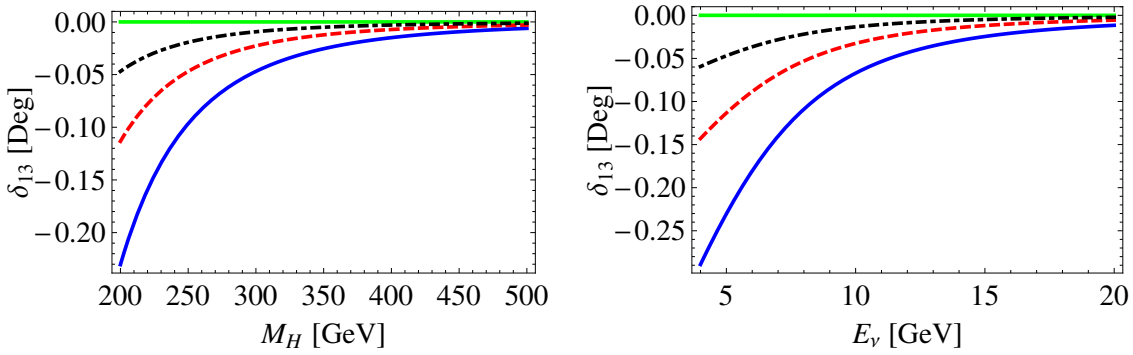

Figure 3.9: Resonance (H): The figures illustrate variation of δ_{13} with M_H (left) and E_ν (right). The green line corresponds to the SM prediction. The black (dotdashed), red (dashed), and blue (solid) lines correspond to $\tan\beta = 40, 50, 60$ at $E_\nu = 5$ GeV (left) and at $M_H = 200$ GeV (right). Here, we use the best-fit value $\theta_{13} = 9.1^\circ$ Ref. (*D.V.Forero and J.W.F.Valle*).

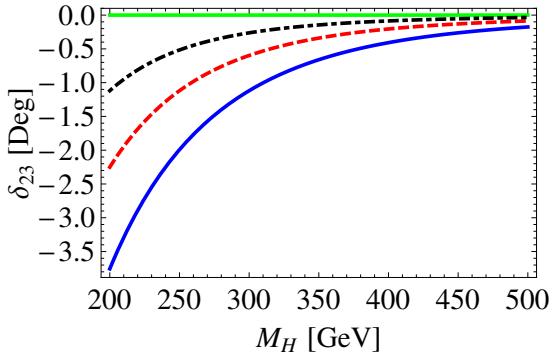

Figure 3.10: Resonance (H): The figures illustrate variation of δ_{23} with M_H. The green line corresponds to the SM prediction. The black (dotdashed), red (dashed), and blue (solid) lines correspond to $\tan\beta = 40, 50, 60$. Here, we use the best-fit value $\theta_{23} = 42.8^\circ$ Ref. (*M.C.Gonzalez-Garcia and J.Salvado*, 2010). We take into account the atmospheric neutrino flux for Kamioka where the Super-Kamiokande experiment locates Ref. (*M.Honda and S.Midorikawa*, 2011).

where I is the 2×2 identity matrix and $\vec{P}$ is the polarization vector of the decaying spin-1/2 lepton.

To determine the components (P_x, P_y, P_z) of the polarization vector we choose the following kinematic variables. The four-momenta of incoming neutrino (k), target nucleon (p) and produced lepton (k') in the laboratory frame are

$$\begin{aligned} k^\mu &= (E_\nu, 0, 0, E_\nu)\,, \\ p^\mu &= (M, 0, 0, 0)\,, \\ k'^\mu &= (E_l, p_l \sin\theta\cos\phi, p_l \sin\theta \sin\phi, p_l \cos\theta)\,. \end{aligned} \tag{3.30}$$

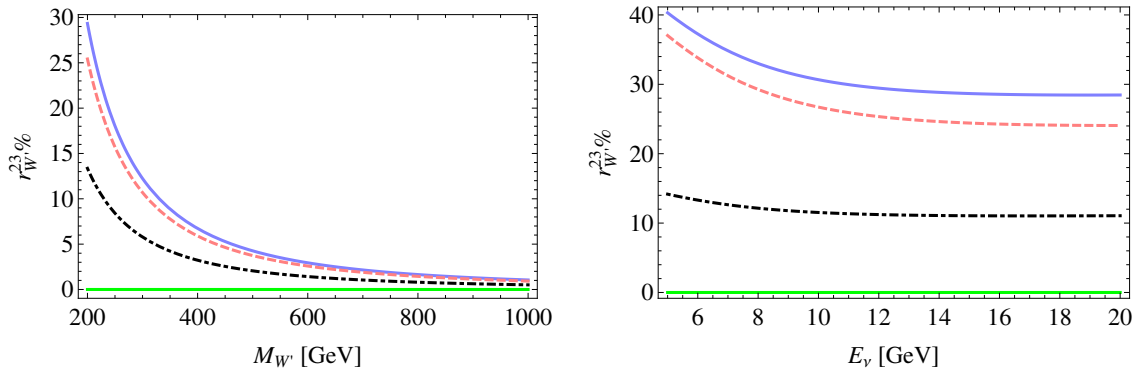

Figure 3.11: Resonance (W'): The left (right) panel figures illustrate the variation of $r^{23}_{W'}\%$ with the W' mass $M_{W'}$ (E_ν) when both left and right-handed W' couplings are present. The lines show predictions for some representative values of the W' couplings $(g_L^{\tau\nu_\tau}, g_L^{ud}, g_R^{ud})$. The green line (solid, lower) corresponds to the SM prediction. The blue line (solid, upper) in the left figure corresponds to (-0.94 , -1.13 , -0.85) at $E_\nu = 17$ GeV, and the blue line (solid, upper) in the right figure corresponds to (1.23 , 0.84 , 0.61) at $M_{W'} = 200$ GeV.

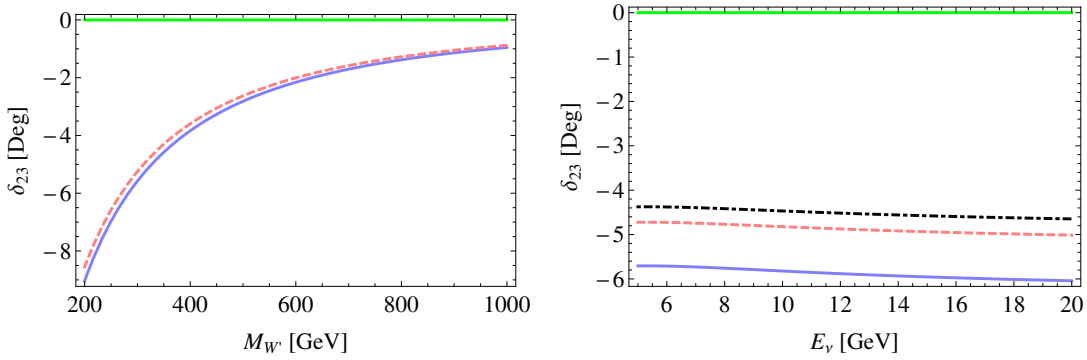

Figure 3.12: Resonance (W'): The left (right) panel figures illustrate the deviation δ_{23} with the W' mass $M_{W'}$ (E_ν) when only left-handed W' couplings are present. The lines show predictions for some representative values of the W' couplings $(g_L^{\tau\nu_\tau}, g_L^{ud})$. The green line (solid, upper) corresponds to the SM prediction. The blue line (solid, lower) in the left figure corresponds to (0.69, 0.89) at $E_\nu = 17$ GeV, and the blue line (solid, lower) in the right figure corresponds to (1.42, 0.22) at $M_{W'} = 200$ GeV. Here, we use the best-fit value $\theta_{23} = 42.8°$ Ref. (*M.C.Gonzalez-Garcia and J.Salvado*, 2010).

We introduce three four-vectors s^a_μ , a = 1, 2, 3 such that the s^a and k'_l/m_l form an orthonormal set of four-vectors as defined in Ref. (*H.E.Haber*, 1994): We choose the three spin four-vectors of the

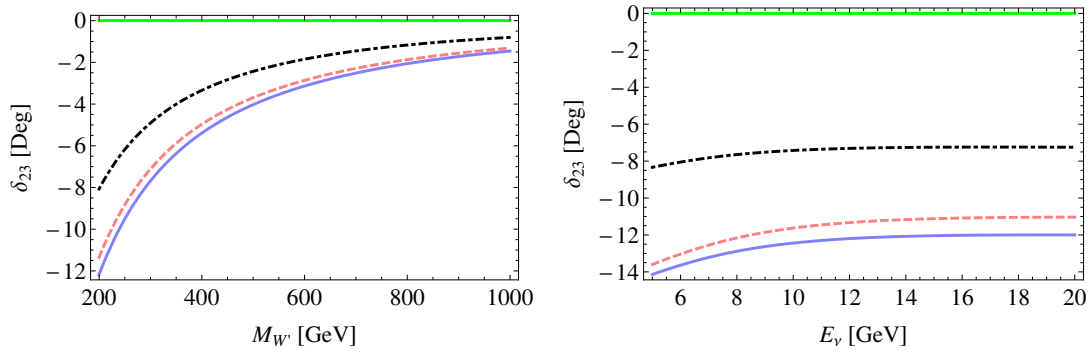

Figure 3.13: Resonance (W'): The left (right) panel figures illustrate the deviation δ_{23} with the W' mass $M_{W'}$ (E_ν) when both left and right-handed W' couplings are present. The lines show predictions for some representative values of the W' couplings $(g_L^{\tau\nu_\tau}, g_L^{ud}, g_R^{ud})$. The green line (solid, upper) corresponds to the SM prediction. The blue line (solid, lower) in the left figure corresponds to (-0.94 , -1.13 , -0.85) at $E_\nu = 17$ GeV, and the blue line (solid, lower) in the right figure corresponds to (1.23 , 0.84 , 0.61) at $M_{W'} = 200$ GeV. Here, we use the best-fit value $\theta_{23} = 42.8°$ Ref. (*M.C.Gonzalez-Garcia and J.Salvado*, 2010).

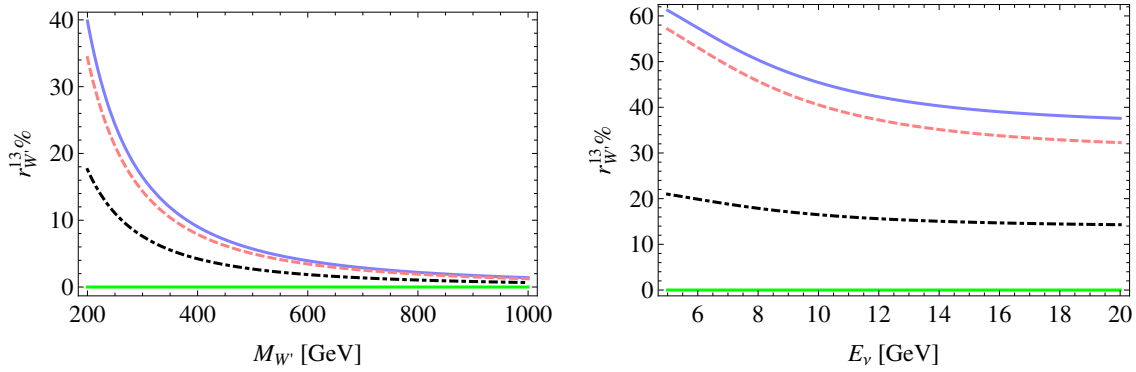

Figure 3.14: Resonance (W'): The left (right) panel figures illustrate the variation of $r_{W'}^{13}\%$ with the W' mass $M_{W'}$ (E_ν) when both left and right-handed W' couplings are present. The lines show predictions for some representative values of the W' couplings $(g_L^{\tau\nu_\tau}, g_L^{ud}, g_R^{ud})$. The green line (solid, lower) corresponds to the SM prediction. The blue line (solid, upper) in the left figure corresponds to (-0.94 , -1.13 , -0.85) at $E_\nu = 17$ GeV, and the blue line (solid, upper) in the right figure corresponds to (1.23 , 0.84 , 0.61) at $M_{W'} = 200$ GeV.

lepton such that

$$\begin{aligned} s^a \cdot k' &= 0, \\ s^a \cdot s^b &= -\delta^{ab}, \\ s^a_\mu \cdot s^b_\nu &= -g_{\mu\nu} + \frac{k'_\mu k'_\nu}{m_l^2}, \end{aligned} \tag{3.31}$$

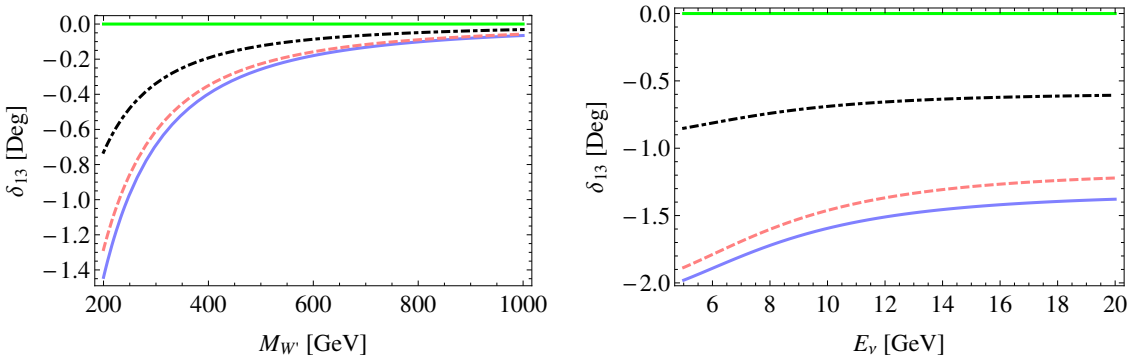

Figure 3.15: Resonance (W'): The left (right) panel figures illustrate the deviation δ_{13} with the W' mass $M_{W'}$ (E_ν) when both left and right-handed W' couplings are present. The lines show predictions for some representative values of the W' couplings $(g_L^{\tau\nu_\tau}, g_L^{ud}, g_R^{ud})$. The green line (solid, upper) corresponds to the SM prediction. The blue line (solid, lower) in the left figure corresponds to (-0.94 , -1.13 , -0.85) at $E_\nu = 17$ GeV, and the blue line (solid, lower) in the right figure corresponds to (1.23 , 0.84 , 0.61) at $M_{W'} = 200$ GeV. Here, we use the best-fit value $\theta_{13} = 9.1^\circ$ Ref. (*D.V.Forero and J.W.F.Valle*).

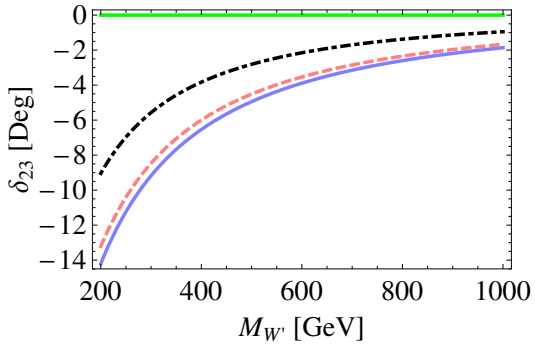

Figure 3.16: Resonance (W'): The figure illustrates the deviation δ_{23} with the W' mass $M_{W'}$ when both left and right-handed W' couplings are present. The lines show predictions for some representative values of the W' couplings $(g_L^{\tau\nu_\tau}, g_L^{ud}, g_R^{ud})$. The green line (solid, upper) corresponds to the SM prediction. The blue line (solid, lower) corresponds to (-0.94 , -1.13 , -0.85). Here, we use the best-fit value $\theta_{23} = 42.8^\circ$ Ref. (*M.C.Gonzalez-Garcia and J.Salvado*, 2010). We take into account the atmospheric neutrino flux for Kamioka where the Super-Kamiokande experiment locates Ref. (*M.Honda and S.Midorikawa*, 2011).

where

$$
\begin{aligned}
s_\mu^1 &= (0, \cos\theta\cos\phi, \cos\theta\sin\phi, -\sin\theta)\,, \\
s_\mu^2 &= (0, -\sin\phi, \cos\phi, 0)\,, \\
s_\mu^3 &= (p_l/m_l, E_l/m_l \sin\theta\cos\phi, E_l/m_l \sin\theta\sin\phi, E_l/m_l \cos\theta)\,. \qquad (3.32)
\end{aligned}
$$

Finally we define the degree of τ polarization P as

$$P = \sqrt{P_x^2 + P_y^2 + P_z^2}. \tag{3.33}$$

The SM results for the polarization components P_x, P_y, P_z can be found in Ref. Ref. (*K. Hagiwara and Yokoya*, 2003) for the DIS. We calculated these components in the presence of the charged Higgs and W' contributions. We computed the degree of τ polarization P with respect to E_τ for 0 degree, 5 degrees and 10 degrees scattering angles with the incident neutrino energy at 10 GeV. In the polarization results we found the charged Higgs and W' model produce tiny deviations from the SM values.

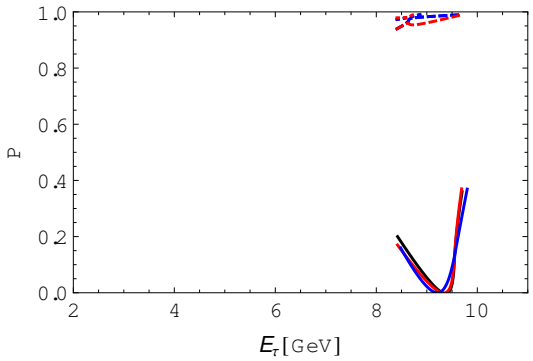

Figure 3.17: Resonance: The figure illustrates the effect of τ-polarization on the resonance scattering

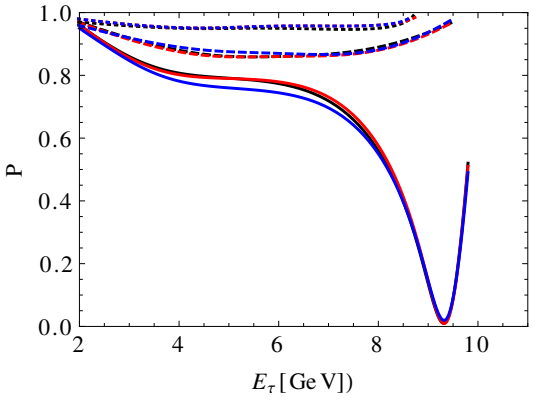

Figure 3.18: DIS: The figure illustrates the effect of τ-polarization on the DIS scattering

3.8 Results

New physics contributions to the tau-neutrino nucleon scattering were considered in this work. We discussed charged Higgs and W' effects to the deep inelastic scattering $\nu_\tau(\bar{\nu}_\tau) + N \to \tau^-(\tau^+) + X$ in the neutrino-nucleon interactions. Considering these effects in the neutrino detection process at neutrino oscillation experiments modify the measured atmospheric and reactor mixing angles θ_{23} and θ_{13}, respectively. The cross section of the deep inelastic scattering was calculated within the range $W_{cut} < W < \sqrt{s} - m_\tau$ with $W_{cut} = 1.4$ GeV. If high-energy LBL experiments could measure θ_{13} via ν_τ appearance, the NP effects can impact the θ_{13} measurement. As θ_{13} is a small angle, large NP parameters are required to produce observable deviations δ_{13}.

In the case of deep inelastic scattering, the charged Higgs contribution does not have interference with the SM cross section. With the constraints on the NP parameters, the NP effects were negligible and the deviations δ_{23} and δ_{13} were very small. The values of deviations were found to be mostly negative in the W' model. The δ_{23} and δ_{13} values increased in magnitude with increasing incident neutrino energy and decreased with increasing $M_{W'}$.

We also considered Δ resonance production $\nu_\tau(\bar{\nu}_\tau) + n(p) \to \tau^-(\tau^+) + \Delta^+(\Delta^0)$ and deep inelastic scattering $\nu_\tau(\bar{\nu}_\tau) + N \to \tau^-(\tau^+) + X$ in the neutrino-nucleon interactions and saw that the deviations are significant.

CHAPTER 4
THE AZIMUTHAL $B \to D^* \tau^- \bar{\nu_\tau}$ ANGULAR DISTRIBUTION WITH TENSORS OPERATORS

4.1 Introduction

The search for new physics (NP) beyond the Standard Model (SM) of particle physics is going on at the energy frontier in colliders such as the LHC and at the intensity frontier at high luminosity experiments. In the intensity frontier, the B factories, BaBar and Belle, have produced an enormous quantity of data and there is still a lot of data to be analyzed from both experiments. The LHCb and Belle II will continue the search for NP through precision measurements in the b quark system. There are a variety of ways in which NP in B decays can be observed Ref. (*A.Datta and D.Ghosh*, 2014; *A.Datta and P.J.O'Donnel*, 2005; *A.Datta*, 2006; *C.-W.Chiang and A.Szynkman*, 2010; *A.Datta and D.London*, 2004a; *S.Baek and D.London*, 2005; *A.Datta and R.Sinha*, 2005). In this NP search, the second and third generation quarks and leptons may be quite special because they are comparatively heavier and could be relatively more sensitive to NP. As an example, in certain versions of the two Higgs doublet models (2HDM) the couplings of the new Higgs bosons are proportional to the masses and so NP effects are more pronounced for the heavier generations. Moreover, the constraints on NP involving, specially the third generation leptons and quarks, are somewhat weaker allowing for larger NP effects Ref. (*A.Rashed and A.Datta*, 2013, 2012; *M.Duraisamy and A.Datta*, 2011; *A.Datta and M.Duraisamy*, 2010; *A.Datta and T.Huang*, 2000).

The semileptonic decays of B meson to the τ lepton is mediated by a W boson in the SM and it is quite well understood theoretically. In many models of NP this decay gets contributions from additional states like new vector bosons, leptoquarks or new scalar particles. These new states can

affect the semileptonic $b \to c$ and $b \to u$ transitions. The exclusive decays $\bar{B} \to D^+\tau^-\bar{\nu_\tau}$ and $\bar{B} \to D^{*+}\tau^-\bar{\nu_\tau}$ are important places to look for NP because, being three body decays, they offer a host of observables in the angular distributions of the final state particles. The theoretical uncertainties of the SM predictions have gone down significantly in recent years because of the developments in heavy-quark effective theory (HQET). The experimental situation has also improved a lot since the first observation of the decay $\bar{B} \to D^{*+}\tau^-\bar{\nu_\tau}$ in 2007 by the Belle Collaboration. After 2007 many improved measurements have been reported by both the BaBar and Belle collaborations and the evidence for the decay $\bar{B} \to D^+\tau^-\bar{\nu_\tau}$ has also been found . Recently, the BaBar collaboration with their full data sample of an integrated luminosity 426 fb^{-1} has reported the measurements of the quantities.

$$\begin{aligned} R(D) &= \frac{BR(\bar{B} \to D^+\tau^-\bar{\nu_\tau})}{BR(\bar{B} \to D^+\ell^-\bar{\nu_\ell})} = 0.440 \pm 0.058 \pm 0.042\,, \\ R(D^*) &= \frac{BR(\bar{B} \to D^{*+}\tau^-\bar{\nu_\tau})}{BR(\bar{B} \to D^*\ell^-\bar{\nu_\ell})} = 0.332 \pm 0.024 \pm 0.018\,, \end{aligned} \tag{4.1}$$

where l denotes the light lepton (e, μ). The SM predictions for $R(D)$ and $R(D^*)$ are Ref. (*S.Fajfer and I.Nisandzic*; *Y.Sakaki and H.Tanaka*)

$$\begin{aligned} R(D) &= 0.297 \pm 0.017\,, \\ R(D^*) &= 0.252 \pm 0.003\,, \end{aligned} \tag{4.2}$$

which deviate from the BaBar measurements by 2σ and 2.7σ respectively. The BaBar collaboration themselves reported a 3.4σ deviation from SM when the two measurements of Eq. (4.1) are taken together. The SLAC BABAR collaboration reports a 3.4 σ excess versus the standard model Ref. (*et al. (BABAR Collaboration)*, 2012) in $\bar{B} \to D^{(*)}\tau^-\nu_\tau$ decay. Belle also has $\bar{B} \to D^{(*)}\tau^-\nu_\tau$ data but it has not yet been completed for publication Ref. (**?**). When Belle FPCP 2013 conference results Ref. (**?**) are added, the excess rises to 4.8 σ. This is currently the largest variance from the Standard Model in collider physics.

These deviations could be sign of NP and already certain models of NP have been considered to explain the data Ref. (*S.Fajfer and I.Nisandzic*; *A.Crivellin and A.Kokulu*, 2012; *A.Datta and D.Ghosh*, 2012; *D.Becirevic and A.Tayduganov*, 2012; *N.G.Deshpande and A.Menon*; *A.Celis and A.Pich*, 2013; *D.Choudhury and A.Kundu*, 2012; *M.Tanaka and R.Watanabe*; *Y.-Y.Fan and Z.-J.Xiao*; *P.Biancofiore and Fazio*; *A.Celis and A.Pich*; *M.Duraisamy and A.Datta*, 2013; *I.Dorner and I.Niandi*, 2013; *Y.Sakaki and R.Watanabe*, 2013). In Ref. Ref. (*A.Datta and D.Ghosh*, 2012), we calculated various observables in $\bar{B} \to D^+\tau^-\bar{\nu_\tau}$ and $\bar{B} \to D^{*+}\tau^-\bar{\nu_\tau}$ decays with NP using an effective Lagrangian approach. The Lagrangian contains two quarks and two leptons scalar, pseudoscalar, vector, axial vector and tensor operators. Considering subsets of the NP operators at a time, the coefficient of these operators can be fixed from the BaBar measurements and then one can study the effect of these operators on the various observables. In Ref. (*M.Duraisamy and A.Datta*, 2013) we extended the work of Ref. (*A.Datta and D.London*, 2004b; *W.Bensalem and D.London*, 2002a,b) by providing the full angular distribution with NP. In particular we focused on the CP violating observables which are the triple product (TP) asymmetries. In the SM these TP's vanish to a very good approximation as the decay is dominated by a single amplitude. Hence, non-zero measurements of these terms are clear signs of NP without any hadronic uncertainties. Note, in the presence of NP with complex couplings the TP's are non-zero and depend on the form factors. Another probe of CP violation using the decay of the τ from $\bar{B} \to D^+\tau^-\bar{\nu_\tau}$ to multipion decays was recently considered Ref. (*K.Hagiwara and Y.Sakaki*).

In this work we included tensor operators in the NP effective Hamiltonian and study their effects on various observables, particularly focusing on the azimuthal observables, including the triple products. Tensor operators were discussed earlier for these decays in Ref. (*M.Tanaka and R.Watanabe*; *P.Biancofiore and Fazio*; *I.Dorner and I.Niandi*, 2013; *Y.Sakaki and R.Watanabe*, 2013). In this work, for $\bar{B} \to D^{*+}\tau^-\bar{\nu_\tau}$, we presented the full three angle and q^2 angular distribution including tensor new physics operators with complex couplings. This represents the full angular distribution with the most general new physics. In our calculations we focused on the effects of the tensor operators on observables that are sensitive to the azimuthal angle χ which

is the angle between the decay plane of the D^* meson and the off-shell W^*. The triple products are the term proportional to the $\sin\chi$ in the angular distribution. For completeness we also discussed other observables such as the q^2 differential distribution as well as the polarization and forward-backward asymmetries.

Finally, we note that tensor operators are often accompanied by other operators in specific NP models. Hence as an example of tensor operators we consider a leptoquark model that has both tensor and scalar operators. Our study showed that the presence of the scalar operators modify the predictions of the different observables in the angular distribution.

4.2 Kinematics

In the B rest frame, the co-ordinates are chosen such that the D^* meson is moving along the positive z-axis, whereas the virtual gauge boson is moving along the negative z-axis. The four-momenta of the B and D^* mesons, and the virtual gauge boson are

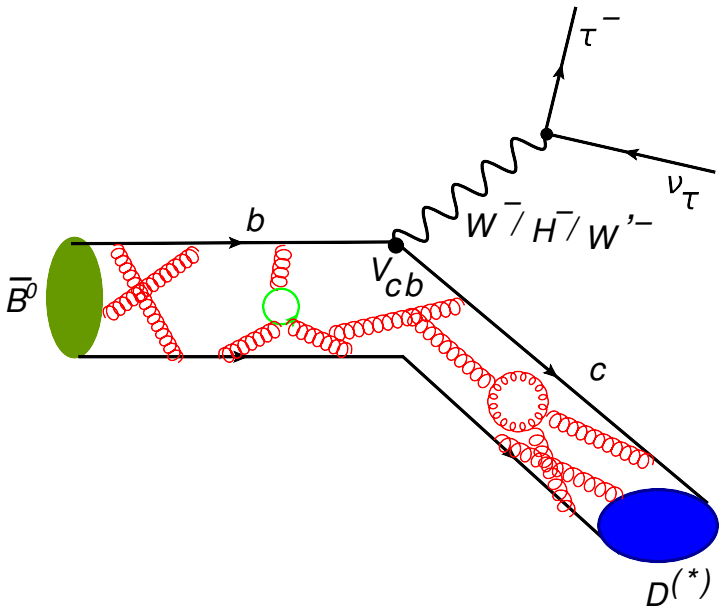

Figure 4.1: The Feynman diagram of $\bar{B} \to D^* \tau^- \nu_\tau$ decay.

$$p_B = (m_B, 0, 0, 0)\,, \;\; p_{D^*} = (E_{D^*}, 0, 0, |p_{D^*}|)\,, \;\; q = (q_0, 0, 0, -|p_{D^*}|)\,, \tag{4.3}$$

where $E_{D^*} = (m_B^2 + m_{D^*}^2 - q^2)/2m_B$, $|p_{D^*}| = \lambda^{1/2}(m_B^2, m_{D^*}^2, q^2)/2m_B$, and $q_0 = (m_B^2 - m_{D^*}^2 + q^2)/2m_B$. Further, one chooses the polarization vector of the D^* meson as

$$\epsilon(0) = \frac{1}{m_{D^*}}(|p_{D^*}|, 0, 0, E_{D^*})\,, \quad \epsilon(\pm) = \mp\frac{1}{\sqrt{2}}(0, 1, \pm i, 0)\,. \tag{4.4}$$

In this frame, we choose the polarization vector of the virtual gauge boson $\bar{\epsilon}$, which can be, longitudinal $(m = 0)$, transverse $(m = \pm)$, or timelike (m = t):

$$\begin{aligned} \bar{\epsilon}(0) &= \frac{1}{\sqrt{q^2}}(|p_{D^{(*)}}|, 0, 0, -q_0)\,, \quad \bar{\epsilon}(\pm) = \frac{1}{\sqrt{2}}(0, \pm 1, -i, 0)\,, \\ \bar{\epsilon}(t) &= \frac{q^\mu}{\sqrt{q^2}} = \frac{1}{\sqrt{q^2}}(q_0, 0, 0, -|p_{D^*}|)\,, \end{aligned} \tag{4.5}$$

The leptonic tensor is evaluated in the q^2 rest frame. In this frame, we choose the transverse components of the helicity basis $\bar{\epsilon}$ to remain the same and other two components are taken as

$$\bar{\epsilon}(0) = (0, 0, 0, -1)\,, \; \bar{\epsilon}(t) = (1, 0, 0, 0)\,. \tag{4.6}$$

Let θ_l be the angle between the three-momenta of D^* meson and the charged lepton in the q^2 rest frame, and χ be the opening angle between the two decay planes. We define the momenta of the lepton and anti-neutrino pairs as

$$\begin{aligned} p_l^\mu &= (E_l, pl\sin\theta_l\cos\chi, pl\sin\theta_l\sin\chi, -pl\cos\theta_l)\,, \\ p_\nu^\mu &= (p_l, -pl\sin\theta_l\cos\chi, -pl\sin\theta_l\sin\chi, pl\cos\theta_l)\,, \end{aligned} \tag{4.7}$$

where the lepton energy $E_l = (q^2 + m_l^2)/2\sqrt{q^2}$ and the magnitude of its three-momenta is $p_l =$

$(q^2 - m_l^2)/2\sqrt{q^2}$.

4.3 Formalism

In the presence of NP, the effective Hamiltonian for the quark-level transition $b \to cl^-\bar{\nu}_l$ can be written in the form

$$\begin{aligned}\mathcal{H}_{eff} &= \frac{4G_F V_{cb}}{\sqrt{2}}\Big[(1+V_L)\,[\bar{c}\gamma_\mu P_L b]\,[\bar{l}\gamma^\mu P_L \nu_l] + V_R\,[\bar{c}\gamma^\mu P_R b]\,[\bar{l}\gamma_\mu P_L \nu_l] \\ &\quad + S_L\,[\bar{c}P_L b]\,[\bar{l}P_L\nu_l] + S_R\,[\bar{c}P_R b]\,[\bar{l}P_L\nu_l] + T_L\,[\bar{c}\sigma^{\mu\nu}P_L b]\,[\bar{l}\sigma_{\mu\nu}P_L\nu_l]\Big], \quad (4.8)\end{aligned}$$

where $G_F = 1.1663787(6) \times 10^{-5} GeV^{-2}$ is the Fermi coupling constant, V_{cb} is the Cabibbo-Kobayashi-Maskawa (CKM) matrix element, $P_{L,R} = (1 \mp \gamma_5)/2$ are the projectors of negative/positive chiralities. We use $\sigma_{\mu\nu} = i[\gamma_\mu, \gamma_\nu]/2$ and assume the neutrino to be always left chiral. Further, we do not assume any relation between $b \to ul^-\nu_l$ and $b \to cl^-\bar{\nu}_l$ transitions and hence do not include constraints from $B \to \tau\nu_\tau$. The SM effective Hamiltonian corresponds to $V_L = V_R = S_L = S_R = T_L = 0$.

4.3.1 $\bar{B} \to D^{*+}\tau^-\bar{\nu_\tau}$ angular distribution

The complete three-angle distribution for the decay $\bar{B} \to D^*(\to D\pi)l^-\bar{\nu}_l$ in the presence of NP can be expressed in terms of four kinematic variables q^2, two polar angles θ_l, θ_{D^*}, and the azimuthal angle χ. The angle θ_l is the polar angle between the charged lepton and the direction opposite to the D^* meson in the $(l\nu_l)$ rest frame. The angle θ_{D^*} is the polar angle between the D meson and the direction of the D^* meson in the $(D\pi)$ rest frame. The angle χ is the azimuthal angle between the two decay planes spanned by the 3-momenta of the $(D\pi)$ and $(l\nu_l)$ systems. These angles are described in Fig. 4.2. The three-angle distribution can be obtained by using the helicity formalism: We can write the angular distribution explicitly for easy comparison with previous literature Ref. (*J.G.Korner*

and G.A.Schuler, 1990, 1989) in terms of the helicity amplitudes

$$\frac{d^4\Gamma}{dq^2\, d\cos\theta_l\, d\cos\theta_{D^*}\, d\chi} = \frac{9}{32\pi} NF\Big(\sum_{i=1}^{8} I_i + \frac{m_l^2}{q^2}\sum_{j=1}^{8} J_i\Big), \tag{4.9}$$

where we can define the I_i and J_i as,

$$
\begin{aligned}
I_1 &= 4\cos^2\theta_{D^*}\Big(\sin^2\theta_l|\mathcal{A}_0|^2 + 8|A_{0T}|^2\Big[1+\cos 2\theta_l\Big]\Big),\\
J_1 &= 4\cos^2\theta_{D^*}\Big(\Big[|\mathcal{A}_0|^2\cos^2\theta_l + |\mathcal{A}_{tP}|^2 - 2Re[\mathcal{A}_{tP}\mathcal{A}_0^*]\cos\theta_l\Big]\\
&\quad +4\Big[|A_{0T}|^2(1-\cos 2\theta_l) - (\frac{m_l^2}{q^2})^{-1/2}Re(\mathcal{A}_{0T}{\mathcal{A}_0}^*)\Big]\Big),\\
I_2 &= \sin^2\theta_{D^*}\Big(\Big[(|\mathcal{A}_\parallel|^2+|\mathcal{A}_\perp|^2)(1+\cos^2\theta_l) - 4Re[\mathcal{A}_\parallel\mathcal{A}_\perp^*]\cos\theta_l\Big]\\
&\quad +8\Big[(|\mathcal{A}_{\parallel_T}|^2+|\mathcal{A}_{\perp T}|^2)(1-\cos^2\theta_l)\Big]\Big),\\
J_2 &= \sin^2\theta_{D^*}\Big(\sin^2\theta_l(|\mathcal{A}_\parallel|^2+|\mathcal{A}_\perp|^2) + 8\Big[(|\mathcal{A}_{\parallel_T}|^2+|\mathcal{A}_{\perp T}|^2)(4+\cos^2\theta_l)\\
&\quad -4Re(\mathcal{A}_{\parallel_T}{\mathcal{A}_{\perp T}}^*)\sin\theta_l - 2(\frac{m_l^2}{q^2})^{-1/2}Re(\mathcal{A}_{\parallel_T}{\mathcal{A}_\parallel}^* + \mathcal{A}_{\perp T}{\mathcal{A}_\perp}^*)(1-\sin\theta_l)\Big]\Big),\\
I_3 &= -\sin^2\theta_{D^*}\sin^2\theta_l\cos 2\chi\Big([|\mathcal{A}_\parallel|^2-|\mathcal{A}_\perp|^2] - 16[|\mathcal{A}_{\parallel_T}|^2-|\mathcal{A}_{\perp T}|^2]\Big),\\
J_3 &= \sin^2\theta_{D^*}\sin^2\theta_l\cos 2\chi\Big([|\mathcal{A}_\parallel|^2-|\mathcal{A}_\perp|^2] - 16(\frac{m_l^2}{q^2})^{-1/2}[|\mathcal{A}_{\parallel_T}|^2-|\mathcal{A}_{\perp T}|^2]\Big),\\
I_4 &= -2\sqrt{2}\sin 2\theta_{D^*}\sin\theta_l\cos\chi Re[\mathcal{A}_\perp\mathcal{A}_0^*],\\
J_4 &= 2\sqrt{2}\sin 2\theta_{D^*}\sin\theta_l\cos\chi\Big(Re[\mathcal{A}_\parallel\mathcal{A}_{tP}^*] - 16\Big[Re(\mathcal{A}_{\perp T}A_{0T}^*)\\
&\quad +(\frac{m_l^2}{q^2})^{-1/2}Re(A_{0T}{\mathcal{A}_\perp}^* + \mathcal{A}_{\perp T}{\mathcal{A}_0}^* - \mathcal{A}_{\parallel_T}A_{tP}^*)\Big]\Big),\\
I_5 &= 2\sqrt{2}\sin 2\theta_{D^*}\sin\theta_l\cos\theta_l\cos\chi\Big(Re[\mathcal{A}_\parallel\mathcal{A}_0^*] - 16Re[\mathcal{A}_{\parallel_T}A_{0T}^*]\Big),\\
J_5 &= -2\sqrt{2}\sin 2\theta_{D^*}\sin\theta_l\cos\theta_l\cos\chi\Big(Re[\mathcal{A}_\parallel\mathcal{A}_0^*] - 16[\mathcal{A}_{\parallel_T}A_{0T}^*]\Big),\\
I_6 &= 2\sin^2\theta_{D^*}\sin^2\theta_l\sin 2\chi Im[\mathcal{A}_\parallel\mathcal{A}_\perp^*],\\
J_6 &= -2\sin^2\theta_{D^*}\sin^2\theta_l\sin 2\chi Im[\mathcal{A}_\parallel\mathcal{A}_\perp^*],\\
I_7 &= -2\sqrt{2}\sin 2\theta_{D^*}\sin\theta_l\sin\chi Im[\mathcal{A}_\parallel\mathcal{A}_0^*],\\
J_7 &= -2\sqrt{2}\sin 2\theta_{D^*}\sin\theta_l\sin\chi\Big(Im[\mathcal{A}_\perp\mathcal{A}_{tP}^*]\\
&\quad -4(\frac{m_l^2}{q^2})^{-1/2}Im(A_{0T}{\mathcal{A}_\parallel}^* - \mathcal{A}_{\parallel_T}A_0^* + \mathcal{A}_{\perp T}A_{tP}^*)\Big),\\
I_8 &= \sqrt{2}\sin 2\theta_{D^*}\sin 2\theta_l\sin\chi Im[\mathcal{A}_\perp\mathcal{A}_0^*],\\
J_8 &= -\sqrt{2}\sin 2\theta_{D^*}\sin 2\theta_l\sin\chi Im[\mathcal{A}_\perp\mathcal{A}_0^*]. \qquad (4.10)
\end{aligned}
$$

The expressions for the hadronic helicity amplitudes can be written in terms of form factors for the $B \to D^*$ matrix elements Ref. (*M.Beneke and T.Feldmann*, 2001)

$$\begin{aligned}
\mathcal{A}_0 &= \frac{(m_B + m_{D^*})}{2m_{D^*}\sqrt{q^2}}\Big[(m_B^2 - m_{D^*}^2 - q^2)A_1(q^2) - \frac{\lambda_{D^*}}{(m_B + m_{D^*})^2}A_2(q^2)\Big](1 - g_A)\,, \\
\mathcal{A}_\pm &= \Big[(m_B + m_{D^*})A_1(q^2)(1 - g_A) \mp \frac{\sqrt{\lambda_{D^*}}}{(m_B + m_{D^*})}V(q^2)(1 + g_V)\Big]\,, \\
\mathcal{A}_t &= \frac{\sqrt{\lambda_{D^*}}}{\sqrt{q^2}}A_0(q^2)(1 - g_A)\,, \\
\mathcal{A}_P &= \frac{\sqrt{\lambda_{D^*}}}{(m_b(\mu) + m_c(\mu))}A_0(q^2)g_P\,, \\
\mathcal{A}_{0T} &= \frac{T_L}{2m_{D^*}}\Big[(m_B^2 + 3m_{D^*}^2 - q^2)T_2(q^2) - \frac{\lambda_{D^*}}{m_B^2 - m_{D^*}^2}T_3(q^2)\Big]\,, \\
\mathcal{A}_{\pm T} &= T_L\Big[\frac{m_B^2 - m_{D^*}^2}{\sqrt{q^2}}T_2(q^2) \pm \sqrt{\frac{\lambda_{D^*}}{q^2}}T_1(q^2)\Big]\,.
\end{aligned} \tag{4.11}$$

The t and the P amplitudes arise in the combination

$$\mathcal{A}_{tP} = \Big(\mathcal{A}_t + \frac{\sqrt{q^2}}{m_\tau}\mathcal{A}_P\Big)\,. \tag{4.12}$$

Further, we define the transversity amplitudes $\mathcal{A}_{\parallel(T)}$ and $\mathcal{A}_{\perp(T)}$ in terms of the helicity amplitudes $\mathcal{A}_{\pm(T)}$ as

$$\begin{aligned}
\mathcal{A}_{\parallel(T)} &= \frac{1}{\sqrt{2}}\left(\mathcal{A}_{+(+T)} + \mathcal{A}_{-(-T)}\right)\,, \\
\mathcal{A}_{\perp(T)} &= \frac{1}{\sqrt{2}}\left(\mathcal{A}_{+(+T)} - \mathcal{A}_{-(-T)}\right)\,.
\end{aligned} \tag{4.13}$$

The expressions for the form factors $A_1(q^2)$, $A_2(q^2)$, $A_0(q^2)$, $V(q^2)$, $T_1(q^2)$, $T_2(q^2)$, and $T_3(q^2)$ in the heavy quark effective theory can be found in Ref. (*A.F.Falk and M.Neubert*, 1993; *Y.Sakaki and*

R.Watanabe, 2013).

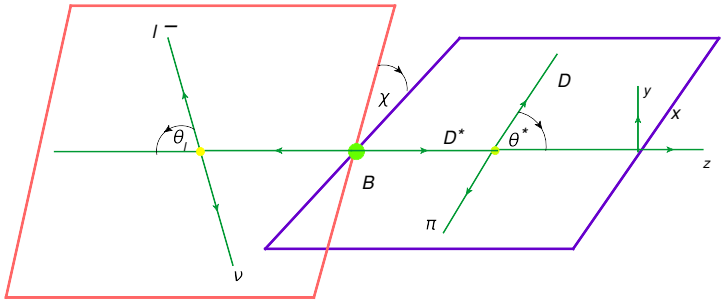

Figure 4.2: The description of the angles θ_{l,D^*} and χ in the angular distribution of $\bar{B} \to D^*(\to D\pi)l^-\nu_l$ decay.

It will be convenient to rewrite the angular distribution as Ref. (*A.K.Alok and D.London*, 2011)

$$\begin{aligned}\frac{d^4\Gamma}{dq^2\, d\cos\theta_l\, d\cos\theta_{D^*}\, d\chi} = \frac{9}{32\pi} NF \Bigg\{ & \cos^2\theta_{D^*}\Big(V_1^0 + V_2^0\cos 2\theta_l + V_3^0\cos\theta_l\Big) \\ & + \sin^2\theta_{D^*}\Big(V_1^T + V_2^T\cos 2\theta_l + V_3^T\cos\theta_l\Big) \\ & + V_4^T\sin^2\theta_{D^*}\sin^2\theta_l\cos 2\chi + V_1^{0T}\sin 2\theta_{D^*}\sin 2\theta_l\cos\chi \\ & + V_2^{0T}\sin 2\theta_{D^*}\sin\theta_l\cos\chi + V_5^T\sin^2\theta_{D^*}\sin^2\theta_l\sin 2\chi \\ & + V_3^{0T}\sin 2\theta_{D^*}\sin\theta_l\sin\chi + V_4^{0T}\sin 2\theta_{D^*}\sin 2\theta_l\sin\chi \Bigg\}\,, \end{aligned} \tag{4.14}$$

where the quantity N_F is

$$N_F = \Big[\frac{G_F^2|p_{D^*}||V_{cb}|^2 q^2}{3\times 2^6\pi^3 m_B^2}\Big(1-\frac{m_l^2}{q^2}\Big)^2 Br(D^*\to D\pi)\Big]\,. \tag{4.15}$$

The momentum of the D^* meson in the B meson rest frame is denoted as $|p_{D^*}| = \lambda^{1/2}(m_B^2, m_{D^{(*)}}^2, q^2)/2m_B$ with $\lambda(a,b,c) = a^2+b^2+c^2-2(ab+bc+ca)$.

The twelve angular coefficients V_i^λ in the $B\to D^*(\to D\pi)l^-\bar{\nu}_l$ angular distribution depend on the couplings, kinematic variables and form factors. The expressions for these coefficients are

given in terms of the hadronic helicity amplitudes of the $\bar{B} \to D^* \tau \bar{\nu}_\tau$ decay and summarized according to the D^* helicity combinations $\lambda_1 \lambda_2$:

The longitudinal V^0's ($\lambda_1 \lambda_2 = 00$) are given by

$$
\begin{aligned}
V_1^0 &= 2\Big[\Big(1+\frac{m_l^2}{q^2}\Big)(|\mathcal{A}_0|^2 + 16|\mathcal{A}_{0T}|^2) + \frac{2m_l^2}{q^2}|\mathcal{A}_{tP}|^2 - \frac{16 m_l}{\sqrt{q^2}}\,\mathrm{Re}[\mathcal{A}_{0T}\mathcal{A}_0^*]\Big]\,, \\
V_2^0 &= 2\Big(1-\frac{m_l^2}{q^2}\Big)\Big[-|\mathcal{A}_0|^2 + 16|\mathcal{A}_{0T}|^2\Big]\,, \\
V_3^0 &= -8\mathrm{Re}[\frac{m_l^2}{q^2}\mathcal{A}_{tP}\mathcal{A}_0^* - \frac{4m_l}{\sqrt{q^2}}\mathcal{A}_{tP}\mathcal{A}_{0T}^*]\,.
\end{aligned}
\tag{4.16}
$$

The transverse V^T's ($\lambda_1 \lambda_2 = ++, --, +-, -+$) are given by

$$
\begin{aligned}
V_1^T &= \Big[\frac{1}{2}\Big(3+\frac{m_l^2}{q^2}\Big)\Big(|\mathcal{A}_\parallel|^2 + |\mathcal{A}_\perp|^2\Big) + 8\Big(1+\frac{3m_l^2}{q^2}\Big)(|\mathcal{A}_{\parallel T}|^2 + |\mathcal{A}_{\perp T}|^2) - \frac{16 m_l}{\sqrt{q^2}}\,\mathrm{Re}[\mathcal{A}_{\parallel T}A_\parallel^* + \mathcal{A}_{\perp T}A_\perp^*]\Big]\,, \\
V_2^T &= \Big(1-\frac{m_l^2}{q^2}\Big)\Big[\frac{1}{2}\Big(|\mathcal{A}_\parallel|^2 + |\mathcal{A}_\perp|^2\Big) - 8(|\mathcal{A}_{\parallel T}|^2 + |\mathcal{A}_{\perp T}|^2)\Big]\,, \\
V_3^T &= 4\mathrm{Re}\Big[-\mathcal{A}_\parallel A_\perp^* - \frac{16m_l^2}{q^2}\mathcal{A}_{\parallel T}\mathcal{A}_{\perp T}^* + \frac{4m_l}{\sqrt{q^2}}\,(\mathcal{A}_{\perp T}\mathcal{A}_\parallel^* + \mathcal{A}_{\parallel T}\mathcal{A}_\perp^*)\Big]\,, \\
V_4^T &= \Big(1-\frac{m_l^2}{q^2}\Big)\Big[-\Big(|\mathcal{A}_\parallel|^2 - |\mathcal{A}_\perp|^2\Big) + 16(|\mathcal{A}_{\parallel T}|^2 - |\mathcal{A}_{\perp T}|^2)\Big]\,, \\
V_5^T &= 2\Big(1-\frac{m_l^2}{q^2}\Big)\mathrm{Im}[\mathcal{A}_\parallel \mathcal{A}_\perp^*]\,.
\end{aligned}
\tag{4.17}
$$

The mixed V^{0T}'s ($\lambda_1 \lambda_2 = 0\pm, \pm 0$) are given by

$$
\begin{aligned}
V_1^{0T} &= \sqrt{2}\Big(1-\frac{m_l^2}{q^2}\Big)\mathrm{Re}[\mathcal{A}_\parallel \mathcal{A}_0^* - 16\mathcal{A}_{\parallel T}\mathcal{A}_{0T}^*]\,, \\
V_2^{0T} &= 2\sqrt{2}\mathrm{Re}\Big[-\mathcal{A}_\perp \mathcal{A}_0^* + \frac{m_l^2}{q^2}\Big(\mathcal{A}_\parallel \mathcal{A}_{tP}^* - 16\mathcal{A}_{\perp T}\mathcal{A}_{0T}^*\Big) + \frac{4m_l}{\sqrt{q^2}}\,\Big(\mathcal{A}_{0T}\mathcal{A}_\perp^* + \mathcal{A}_{\perp T}\mathcal{A}_0^* - \mathcal{A}_{\parallel T}\mathcal{A}_{tP}^*\Big)\Big]\,, \\
V_3^{0T} &= 2\sqrt{2}\mathrm{Im}\Big[-\mathcal{A}_\parallel \mathcal{A}_0^* + \frac{m_l^2}{q^2}\mathcal{A}_\perp \mathcal{A}_{tP}^* + \frac{4m_l}{\sqrt{q^2}}\,(\mathcal{A}_{0T}\mathcal{A}_\parallel^* - \mathcal{A}_{\parallel T}\mathcal{A}_0^* + \mathcal{A}_{\perp T}\mathcal{A}_{tP}^*)\Big]\,, \\
V_4^{0T} &= \sqrt{2}\Big(1-\frac{m_l^2}{q^2}\Big)\mathrm{Im}[\mathcal{A}_\perp \mathcal{A}_0^*]\,.
\end{aligned}
\tag{4.18}
$$

We used HQET to expand the form factors in terms of certain parameters, which are then fixed from the angular distribution for $B \to D^* \ell^- \bar{\nu}_\ell$, where $\ell = e, \mu$. Our basis assumption was that $B \to D^* \ell^- \bar{\nu}_\ell$ decays are described by the SM.

The following single-differential angular distributions allow access to various observables that can be used to probe for NP. The differential decay rate $d\Gamma/dq^2$ obtained after performing integration over all the angles

$$\frac{d\Gamma}{dq^2} = \frac{3N_F}{4}(A_L + A_T)\,. \tag{4.19}$$

Here the D^* meson's longitudinal and transverse polarization amplitudes A_L and A_T are

$$A_L = \Big(V_1^0 - \frac{1}{3}V_2^0\Big), \quad A_T = 2\Big(V_1^T - \frac{1}{3}V_2^T\Big)\,. \tag{4.20}$$

Furthermore, one can also explore the q^2 dependent of ratio

$$R_{D^*}(q^2) = \frac{dBr[\bar{B} \to D^{*+}\tau^-\bar{\nu_\tau}]/dq^2}{dBr[\bar{B} \to D^*\ell^-\bar{\nu_\ell}]/dq^2}\,. \tag{4.21}$$

By integrating out the polar angles θ_l, θ_{D^*}, and the azimuthal angle χ in different kinematic regions, various 2-fold angular distributions can be obtained. For a detailed discussion see Ref. (*M.Duraisamy and A.Datta*, 2013). Here, we have updated these angular distributions with the new tensor couplings. Our results agree with the corresponding angular distributions in Ref. (*Y.Sakaki and R.Watanabe*, 2013). Several observables can be defined through the 2-fold angular distributions. The D^* polarization fraction F_L, the forward-backward asymmetry A_{FB} for the leptons, the azimuthal asymmetries, including the three transverse asymmetries $A_C^{(1,2,3)}$, and the three T-odd CP asymmetries $A_T^{(1,2,3)}$, are defined in terms of angular coefficients $V_i's$

Ref. (*M.Duraisamy and A.Datta*, 2013):

$$
\begin{aligned}
F_L^{D^*}(q^2) &= \frac{A_L}{A_L + A_T} & A_{FB}^{D^*}(q^2) &= \frac{V_3^T + \frac{1}{2}V_3^0}{A_L + A_T}, \\
A_C^{(1)}(q^2) &= \frac{4V_4^T}{3(A_L + A_T)} & A_T^{(1)}(q^2) &= \frac{4V_5^T}{3(A_L + A_T)}, \\
A_C^{(2)}(q^2) &= \frac{V_2^{0T}}{(A_L + A_T)} & A_T^{(2)}(q^2) &= \frac{V_3^{0T}}{(A_L + A_T)}, \\
A_C^{(3)}(q^2) &= \frac{V_1^{0T}}{(A_L + A_T)} & A_T^{(3)}(q^2) &= \frac{V_4^{0T}}{(A_L + A_T)}.
\end{aligned} \tag{4.22}
$$

.

In closing this section we note that even though we are focused on the $\bar{B} \to D^{*+}\tau^-\bar{\nu_\tau}$ decay the $\bar{B} \to D^+\tau^-\bar{\nu_\tau}$ decay is used to constrain the NP operators. The $\bar{B} \to D^+\tau^-\bar{\nu_\tau}$ angular distribution, with tensor operators, can be written as,

$$
\begin{aligned}
\frac{d\Gamma^D}{dq^2 d\cos\theta_l} &= 2N_D|p_D| \left[|H_0|^2 \sin^2\theta_l + \frac{m_l^2}{q^2}(H_0\cos\theta_l - H_{tS})^2 \right. \\
&\left. +8\left(\left((1+\frac{m_l^2}{q^2}) + (1-\frac{m_l^2}{q^2})\cos 2\theta_l\right)|H_T|^2 - \frac{m_l}{\sqrt{q^2}} Re[H_T(H_0^* - H_{tS}^*\cos\theta_l)] \right) \right],
\end{aligned} \tag{4.23}
$$

where the prefactor $N_D = \frac{G_F^2|V_{cb}|^2 q^2}{256\pi^3 m_B^2}\left(1 - \frac{m_l^2}{q^2}\right)^2$. The helicity amplitudes are

$$
\begin{aligned}
H_0 &= \sqrt{\frac{\lambda_D}{q^2}}(1+g_V)F_+(q^2)\,, \quad H_t = \frac{m_B^2 - m_D^2}{\sqrt{q^2}}(1+g_V)F_0(q^2)\,, \\
H_S &= -\frac{m_B^2 - m_D^2}{m_b(\mu) - m_c(\mu)}\, g_S\, F_0(q^2)\,, \quad H_T = -\frac{\sqrt{\lambda_D}}{m_B + m_D}\, T_L\, F_T(q^2)\,,
\end{aligned} \tag{4.24}
$$

where $g_{V,A} = V_R \pm V_L$ and $g_{S,P} = S_R \pm S_L$. In addition, the H_t and the H_S amplitudes arise in the combination,

$$
H_{tS} = \left(H_t - \frac{\sqrt{q^2}}{m_\tau} H_S\right). \tag{4.25}
$$

4.4 An Explicit Model

Many extensions of the SM, motivated by a unified description of quarks and leptons, predict the existence of new scalar and vector bosons, called leptoquarks, which decay into a quark and a lepton. These particles carry nonzero baryon and lepton numbers, color and fractional electric charges. The most general dimension four $SU(3)_c \times SU(2)_L \times U(1)_Y$ invariant Lagrangian of leptoquarks satisfying baryon and lepton number conservation was considered in Ref Ref. (*W.Buchmuller and D.Wyler*, 1987). As the tensor operators in the effective Lagrangian get contributions only from scalar leptoquarks, we have focused only on scalar leptoquarks and considered the case where the leptoquark is a weak doublet or a weak singlet. The weak doublet leptoquark, R_2 has the quantum numbers $(3, 2, 7/6)$ under $SU(3)_c \times SU(2)_L \times U(1)_Y$ while the singlet leptoquark S_1 has the quantum numbers $(\bar{3}, 1, 1/3)$.

The interaction Lagrangian that induces contributions to the $b \to c\ell\overline{\nu}$ process is Ref. (*M.Tanaka and R.Watanabe*)

$$\begin{aligned} \mathcal{L}_2^{\rm LQ} &= \left(g_{2L}^{ij}\,\overline{u}_{iR} R_2^T L_{jL} + g_{2R}^{ij}\,\overline{Q}_{iL} i\sigma_2 \ell_{jR} R_2\right), \\ \mathcal{L}_0^{\rm LQ} &= \left(g_{1L}^{ij}, \overline{Q}_{iL}^c i\sigma_2 L_{jL} + g_{1R}^{ij}, \overline{u}_{iR}^c \ell_{jR}\right) S_1, \end{aligned} \tag{4.26}$$

where Q_i and L_j are the left-handed quark and lepton $SU(2)_L$ doublets respectively, while u_{iR}, d_{iR} and ℓ_{jR} are the right-handed up, down quark and charged lepton $SU(2)_L$ singlets. Indices i and j denote the generations of quarks and leptons, and $\psi^c = C\overline{\psi}^T = C\gamma^0\psi^*$ is a charge-conjugated fermion field. The fermion fields are given in the gauge eigenstate basis and one should make the transformation to the mass basis. Assuming the quark mixing matrices to be hierarchical, and considering only the leading contribution we can ignore the effect of mixing. After performing the Fierz transformations,we found the general Wilson coefficients at the leptoquark mass scale

contributing to the $b \to c\tau\overline{\nu}_l$ process:

$$\begin{aligned} S_L &= \frac{1}{2\sqrt{2}G_F V_{cb}} \left[-\frac{g_{1L}^{33} g_{1R}^{23*}}{2M_{S_1}^2} - \frac{g_{2L}^{23} g_{2R}^{33*}}{2M_{R_2}^2} \right], \\ T_L &= \frac{1}{2\sqrt{2}G_F V_{cb}} \left[\frac{g_{1L}^{33} g_{1R}^{23*}}{8M_{S_1}^2} - \frac{g_{2L}^{23} g_{2R}^{33*}}{8M_{R_2}^2} \right]. \end{aligned} \tag{4.27}$$

It is clear from Eq. (4.27) that the weak singlet leptoquark and the weak doublet can add constructively or destructively to the Wilson's coefficients of the scalar and tensor operators in the effective Hamiltonian. We considered various scenarios. In the first case the singlet and the doublet scalar leptoquark couplings are such that the scalar operator couplings are enhanced and the tensor operator couplings are suppressed. This scenarios has been studied before Ref. (*A.Datta and D.Ghosh*, 2012; *M.Duraisamy and A.Datta*, 2013). Hence, the first case, called Case. (a), we studied that when the tensor operators is enhanced and the scalar operator suppressed. The results of the pure tensor coupling are presented in the next section.

In this section we also considered the possibilities where both the scalar and the tensor operators are present and are of similar sizes. In the most general case both the singlet and doublet leptoquarks are present and so both the scalar and tensor operators appear in the effective Hamiltonian. As there is limited experimental information, including both the singlet and the doublet leptoquarks will allow us more flexibility in fitting for the Wilson's coefficients but this will come with the price of less precise predictions for the various observables. We, therefore, considered the simpler cases when only a singlet or a doublet leptoquark are present. In these cases, from Eq. (4.27) the coefficients of scalar operators and the tensor operators have the same magnitudes. We considered further two cases:

Case. (b): In this case only the weak doublet scalar leptoquark R_2 is present. It was shown recently Ref. (*J.M.Arnold and M.B.Wise*, 2013) that this is one of the two minimal renormalizable scalar leptoquark model, where the standard model is augmented only by one additional scalar representation of $SU(3) \times SU(2) \times U(1)$ and which do not allow proton decay at the tree level.

The relations between the scalar and tensor couplings in Eq.4.27 are valid at the leptoquark

mass scale, $m_{\rm LQ}$. We have to run them down to the b quark mass scale using the scale dependence of the scalar and tensor currents at leading logarithm approximation

$$S_L(\mu_b) = \left[\frac{\alpha_s(m_t)}{\alpha_s(\mu_b)}\right]^{\frac{\gamma_S}{2\beta_0^{(5)}}} \left[\frac{\alpha_s(m_{\rm LQ})}{\alpha_s(m_t)}\right]^{\frac{\gamma_S}{2\beta_0^{(6)}}} S_L(m_{\rm LQ})\,, \tag{4.28}$$

$$T_L(\mu_b) = \left[\frac{\alpha_s(m_t)}{\alpha_s(\mu_b)}\right]^{\frac{\gamma_T}{2\beta_0^{(5)}}} \left[\frac{\alpha_s(m_{\rm LQ})}{\alpha_s(m_t)}\right]^{\frac{\gamma_T}{2\beta_0^{(6)}}} T_L(m_{\rm LQ})\,, \tag{4.29}$$

where the anomalous dimensions of the scalar and tensor operators are $\gamma_S = -6C_F = -8$, $\gamma_T = 2C_F = 8/3$ respectively and $\beta_0^{(f)} = 11 - 2n_f/3$ Ref. (*I.Dorner and I.Niandi*, 2013). Choosing a value for the leptoquark mass we can run the couplings to the b-quark scale which is chosen to be $\mu_b = \overline{m}_b = 4.2$ GeV.

In the simplified scenario with the presence of only one type of leptoquark, namely R_2 or S_1, the scalar S_L and tensor T_L Wilson coefficients are no longer independent: one finds that at the scale of leptoquark mass, $m_{\rm LQ}$, $S_L(m_{\rm LQ}) = \pm T_L(m_{\rm LQ})$. Then, using Eq. (4.29), one obtains the relation at the bottom mass scale,

$$S_L(\overline{m}_b) \simeq \pm 7.8\, T_L(\overline{m}_b)\,. \tag{4.30}$$

for a leptoquark mass of 1 TeV Ref. (*M.Tanaka and R.Watanabe*).

It is interesting to note that the same coupling that appears in the process $b \to c\tau\overline{\nu}_l$ also appears in the $t \to c\tau^+\tau^-$ decay and if the components of the doublet leptoquark have the same mass, then we had a prediction for this decay based on data from $B \to D^{(*)}\tau\overline{\nu}_\tau$ transition.

Case. (c): In this case only the singlet leptoquark is present and the relevant Wilson's coefficients can be obtained from Eq. (4.27).

4.5 Numerical analysis

The model independent and dependent numerical results for the various observables in the angular distribution of $\bar{B} \to D^{*+}\tau^-\bar{\nu_\tau}$ decay are discussed in this section.

4.5.1 Model independent results

For the numerical calculation, we use the $B \to D$ and $B \to D^*$ form factors in the heavy quark effective theory(HQET) framework Ref. (*I.Caprini and M.Neubert*, 1998). A detailed discussions on the $B \to D^*$ and $B \to D$ form factors and their numerical values can be found in Ref. (*Y.Sakaki and R.Watanabe*, 2013). The constraints on the complex NP couplings in the $b \to cl^-\bar{\nu}_l$ effective Hamiltonian come from the measured $R(D)$ and $R(D^*)$ in Eq. (4.1) at 95% C.L. We varied the free parameters in the HQET form factors within their error bars. All the other numerical values were taken from Ref. (*PDG*, 2010) and Ref. (*HFAG*, 2010). The allowed ranges for the NP couplings were then used for predicting the possible allowed ranges for the observables.

It is important to point out that the combination of couplings $g_V = V_R + V_L$ appears in both $R(D)$ and $R(D^*)$, while $g_A = V_R - V_L$ appears only in $R(D^*)$. V_R and V_L receive constraints from both $R(D)$ and $R(D^*)$. While, the combination of couplings $g_S = S_R + S_L$ appears only in $R(D)$, $g_P = S_R - S_L$ appears only in $R(D^*)$. If NP is established in both $R(D)$ and $R(D^*)$ then the cases of pure g_A or g_S or g_P coupling are ruled out. A detailed discussions on the effects of vector and scalar couplings on the various observables in the decays $\bar{B} \to D^*\ell^-\bar{\nu}_\ell$ and $\bar{B} \to D^+\ell^-\bar{\nu}_\ell$ can be found in Ref. (*A.Datta and D.Ghosh*, 2012; *M.Duraisamy and A.Datta*, 2013).

We first considered the Case. (a) of the previous section where only the NP tensor operator is present in the effective Hamiltonian. In Fig. (4.3), the constraint on the parameter space of the pure tensor coupling by both $R(D)$ and $R(D^*)$ measurements at 95% C.L. is shown. We found that the magnitude of tensor coupling satisfies $|T_L| < 0.5$.

The predictions for the differential branching ratio (DBR), $F_L^{D^*}(q^2)$, $R(D^*)(q^2)$ and $A_{FB}^{D^*}(q^2)$ are shown in Fig. (4.4) for the allowed values of tensor coupling. It is clear that, the DBR, $F_L^{D^*}(q^2)$, and $R(D^*)(q^2)$ get considerable deviation from their SM expectation in this new physics scenario. The contribution of pure tensor coupling to the forward-backward asymmetry is of the order of $m_\tau/\sqrt{q^2}$, and $A_{FB}^{D^*}(q^2)$ behaves similar to its SM expectation.

We now analyzed the sensitivity of the q^2-integrated azimuthal symmetries on the new tensor coupling, and we presented correlations of these symmetries with respect to the integrated forward-

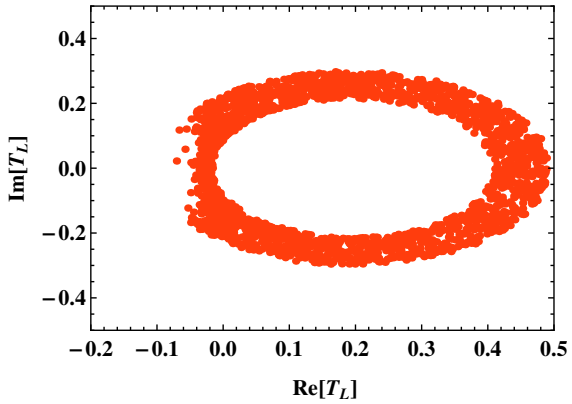

Figure 4.3: The allowed region for the complex coupling T_L for Case. (a) at 95% C.L.

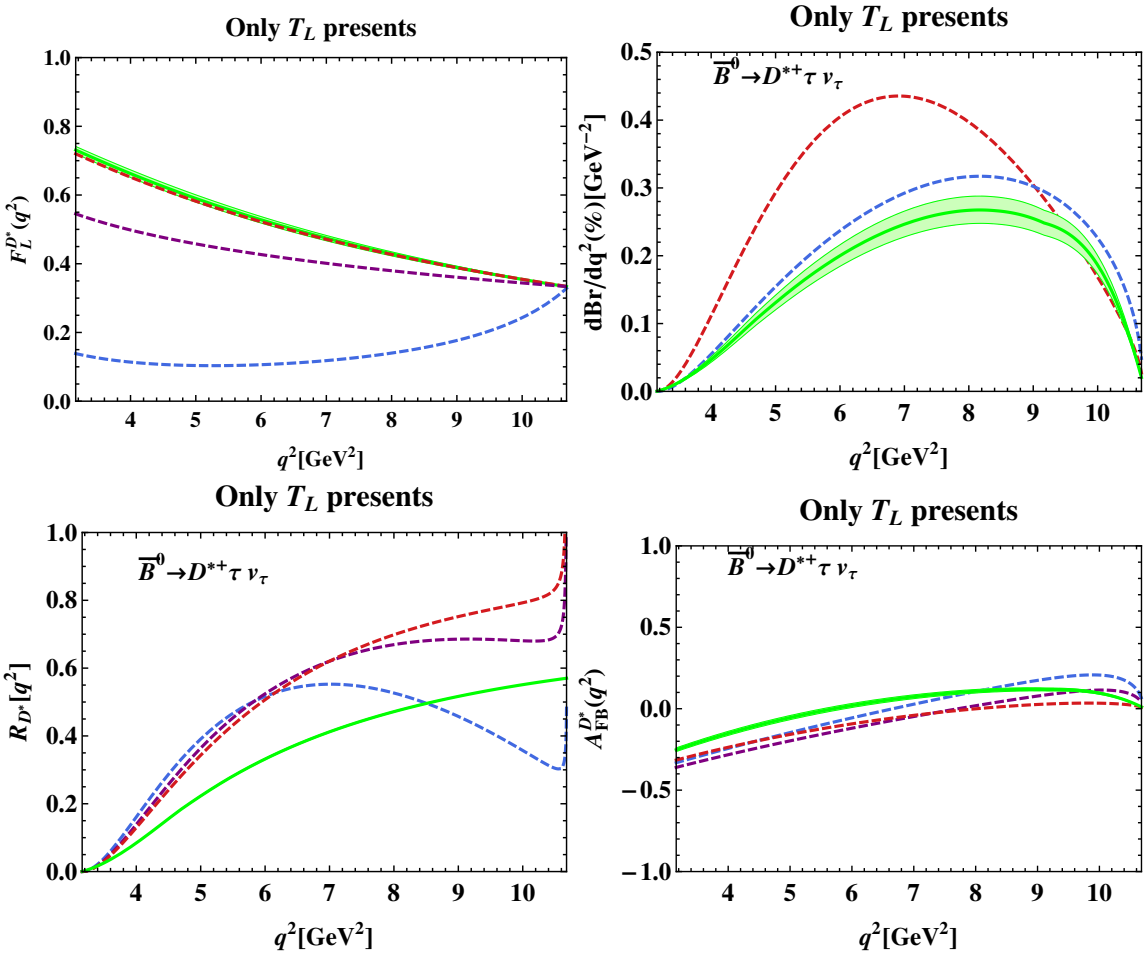

Figure 4.4: The predictions for the observables $F_L^{D^*}(q^2)$, differential branching ratio, $R_{D^*}(q^2)$, and $A_{FB}^{D^*}(q^2)$ for the decay $\bar{B}^0 \to D^{*+}\tau\nu_\tau$ in the presence of only T_L coupling. The green band corresponds to the SM prediction and its uncertainties. The values of the coupling T_L were chosen to show the maximum and minimum deviations from the SM expectations.

backward asymmetry (FBA). The q^2-integrated FBA $< A_{FB}^{D^*} >$, the three transverse asymmetries $< A_C^{(1,2,3)} >$, and the three T-odd CP asymmetries $< A_T^{(1,2,3)} >$ were obtained by separately integrating out the q^2-dependence in the numerator and denominator of these quantities as expressed in Eq.(4.22). The panels of Fig.(4.5) show the correlation between the above six q^2-integrated asymmetries and $< A_{FB} >$ for the decay $\bar{B}^0 \to D^{*+}\tau\nu_\tau$. Note that, in this plot we also included predictions for the vector and scalar NP couplings. In each cases, the NP couplings satisfy the current measurements of R_D and R_{D^*} at 95% C.L. It is clear from these plots that $< A_{FB}^{D^*} >$, and $< A_C^{(1,2,3)} >$ get considerable deviations from their SM expectation once we include the NP couplings. The T-odd CP asymmetry $< A_T^{(2)} >$ is sensitive to all NP couplings, and is strongly correlated with $< A_{FB}^{D^*} >$. The scalar NP couplings can enhance this asymmetry about 5% from its SM value. On the other hand, $< A_T^{(1)} >$ and $< A_T^{(3)} >$ are only sensitive to the vector couplings. These asymmetries are also strongly correlated with $< A_{FB}^{D^*} >$ in the presence of vector NP couplings, and can be enhanced up to 3% from its SM value. Hence, the predictions for $< A_{FB}^{D^*} >$ and azimuthal symmetries have varying sensitivities to the different NP scenarios and these observables were powerful probes of the structure of NP.

4.5.2 Leptoquark model results

We next move to Case.(b) and Case.(c) for the leptoquark with the mass scale of the order of 1 TeV. The allowed ranges for the leptoquark couplings at $\mu = m_b$ from the measured $R(D)$ and $R(D^*)$ values within the 2σ level are shown in Fig. (4.6). These results suggest that the magnitudes of the doublet and singlet leptoquark effective couplings, $g_{2L}^{23} g_{2R}^{33*}$ and $g_{1L}^{33} g_{1R}^{23*}$ are of $O(1)$. A similar conclusion is obtained in Ref. (*Y.Sakaki and R.Watanabe*, 2013).

The correlations between the asymmetries $< A_C^{(1,2,3)} >$ and $< A_T^{(2)} >$ and R_{D^*} are shown in Fig. (4.7) for three different NP scenarios: only S_L, only R_2 leptoquark ($S_L = 7.8 T_L$), and only S_1 leptoquark ($S_L = -7.8 T_L$). These results imply that $< A_C^{(1,2,3)} >$ and $< A_T^{(2)} >$ can get sizeable contributions from the leptoquarks within the measured region of R_{D^*}. It is interesting to note that the behavior of $< A_C^{(2)} >$ is different for R_2 and S_1 leptoquark couplings. Hence this observable

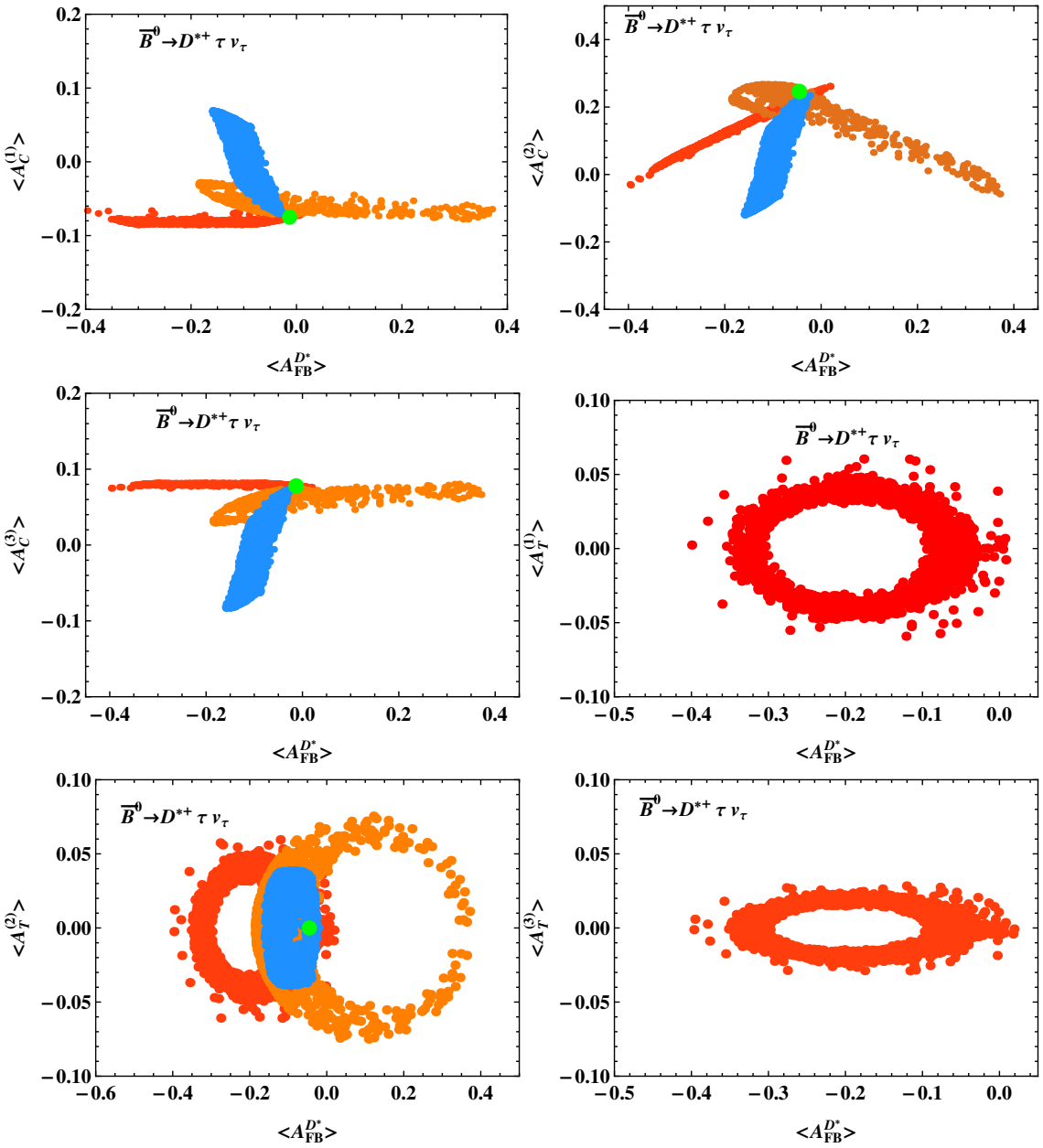

Figure 4.5: The correlation plots between $< A_C^{(1,2,3)} >$ ($< A_T^{(1,2,3)} >$) and $< A_{FB}^{D^*} >$ in the presence of complex NP couplings. The red, orange and blue scatter points correspond to pure vector NP couplings (V_L, V_R), pure scalar NP couplings (S_L, S_R) , and pure tensor NP coupling (T_L). The scatter points are allowed by measurements of R_D and R_{D^*} at 95% C.L. The green points correspond to the SM predictions for these quantities.

can be used to discriminate between the singlet and the doublet leptoquark models.

In Fig.(4.8) we plotted the correlations of $< A_C^{(1,2,3)} >$ and $< A_T^{(2)} >$ with $< A_{FB}^{D^*} >$ in the presence of R_2 and S_1 leptoquark contributions. In each case, the constraints on the leptoquark

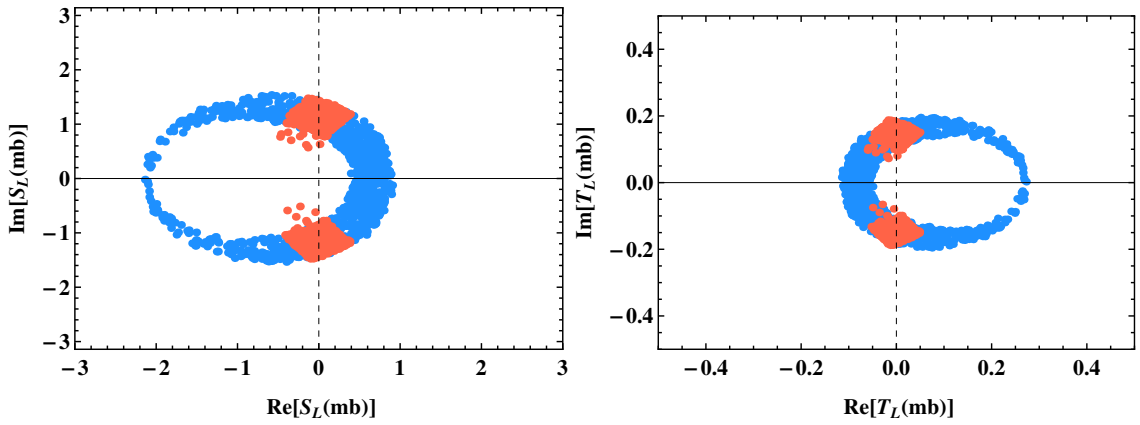

Figure 4.6: The allowed regions for the leptoquark effective couplings S_L and T_L at $\mu_b = 4.2GeV$. The constraints on these NP couplings are from the measured $R(D)$ and $R(D^*)$ within the 2σ level. The red (blue) scatter points correspond to $S_1(R_2)$ leptoquark models.

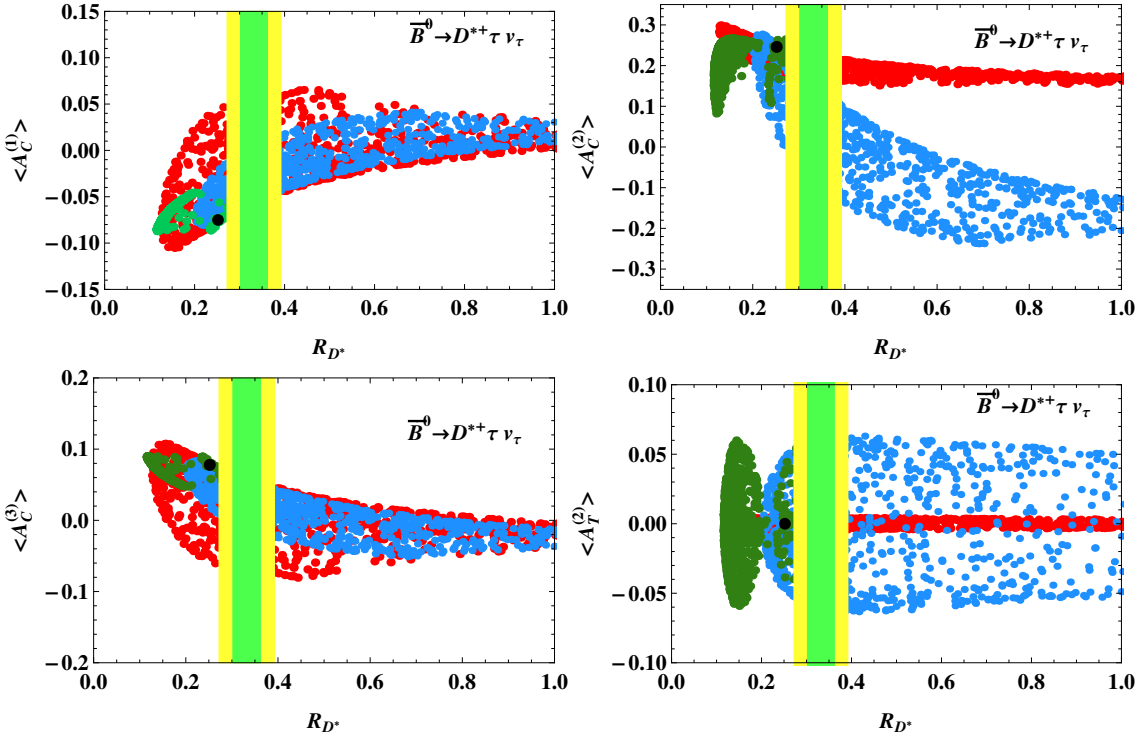

Figure 4.7: The correlations between $< A_C^{(1,2,3)} >$ ($< A_T^{(2)} >$) and R_{D^*} for three different NP scenarios: only S_L coupling (green), R_2 leptoquark coupling (red), and S_1 leptoquark coupling (blue). The black points correspond to the SM predictions for these quantities. The vertical bands correspond to R_{D^*} data with $\pm 1\sigma$ (green) or $\pm 2\sigma$ (yellow) errors.

couplings at $\mu = m_b$ were from the current measurements of R_D and R_{D^*} within the 2 σ level.

As in the case of pure tensor couplings, these plots show that the different leptoquark models

produce very different predictions for the azimuthal asymmetries and so these observables were very sensitive in ruling out different leptoquark models.

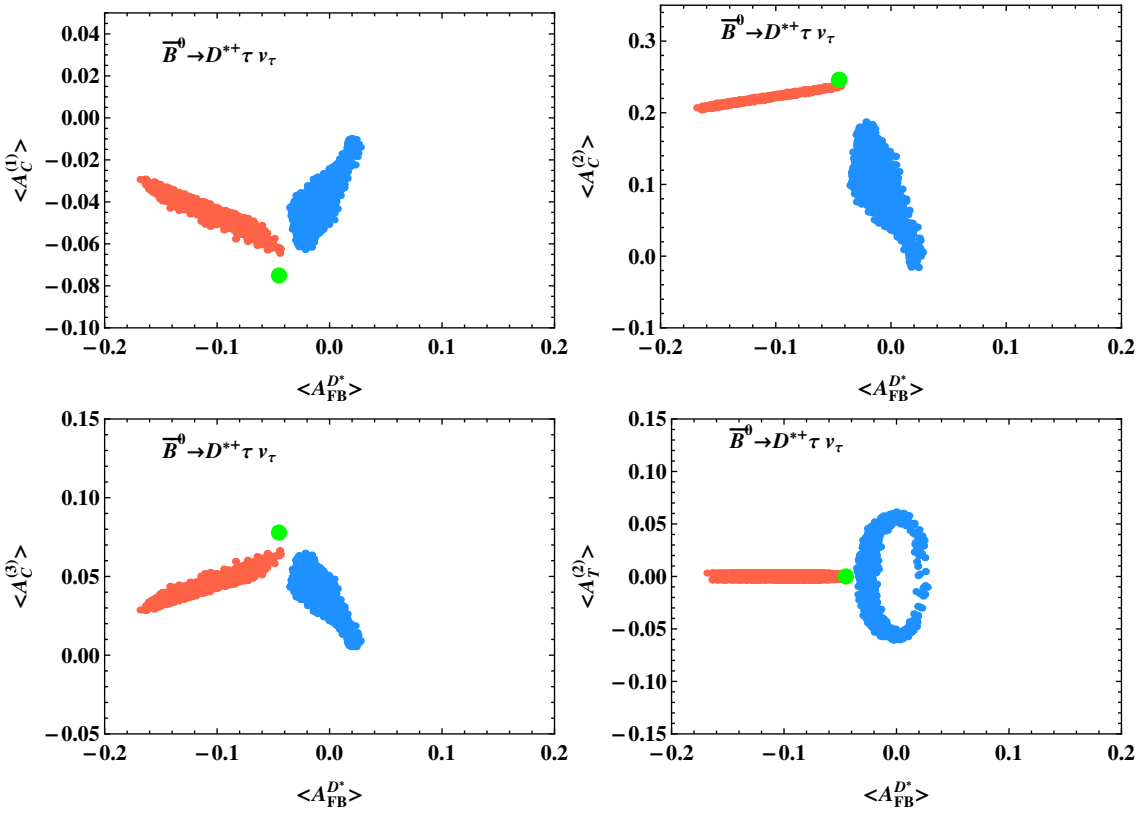

Figure 4.8: The correlation plots between $< A_C^{(1,2,3)} >$, $< A_T^{(2)} >$, and $< A_{FB}^{D^*} >$ in the presence of leptoquark contributions. The red (blue) scatter points correspond to $R_2(S_1)$ leptoquarks. These scatter points satisfy the current measurements of R_D and R_{D^*} within the 2 σ level. The green points in each panel correspond to the SM predictions for these quantities.

4.6 Results and Summary

In summary we have discussed the effects of tensor operators in the decay $\bar{B} \to D^{*+}\tau^-\bar{\nu_\tau}$ motivated by recent measurements which show deviation from the SM predictions in $\bar{B} \to D^{*+}\tau^-\bar{\nu_\tau}$ and $\bar{B} \to D^{+}\tau^-\bar{\nu_\tau}$. In this work we have presented the angular distribution for $\bar{B} \to D^{*+}\tau^-\bar{\nu_\tau}$ with the most general new physics structure including tensor operators. We have then discussed the effects of the tensor operators on various observables that can be constructed out of the angular distribution. Our focus was on the azimuthal observables which include the important CP

violating triple product asymmetries. We found that these azimuthal asymmetries, integrated over q^2, have different sensitivities to different NP structures and hence they can be powerful probes of the nature of the NP. These asymmetries also show strong correlations with the q^2 integrated forward-backward asymmetry. Tensor operators naturally arise in scalar leptoquark models and are accompanied by other scalar operators. We considered two leptoquark models where the leptoquarks are weak singlets and doublets. We discussed the predictions for the azimuthal observables in these models and found that these observables are very efficient in discriminating between the two leptoquark models. In particular we found that there is cancellation between the scalar and tensor components in the scalar doublet leptoquark model for one of the triple product asymmetries while this is not the case for the scalar singlet leptoquark model.

CHAPTER 5
NEW PHYSICS IN $\Lambda_b \to \Lambda_c \tau \nu_\tau$

5.1 Introduction

In this work we worked out the details of the decay process $\Lambda_b \to \Lambda_c \tau \nu_\tau$ within the standard model as done in Ref. (*Körner and Kramer*, 1992) and Ref. (*Datta*, 1994) and with we have included new physics parameters also. Our aim was to look at the deviation from standard model physics.

5.2 Formalism

The Hamiltonian can be written as

$$\begin{aligned}\mathcal{H}_{eff} &= \frac{4G_F V_{cb}}{\sqrt{2}}\Big[(1+V_L)\,[\bar{c}\gamma_\mu P_L b]\,[\bar{l}\gamma^\mu P_L \nu_l] + V_R\,[\bar{c}\gamma^\mu P_R b]\,[\bar{l}\gamma_\mu P_L \nu_l] \\ &\quad + S_L\,[\bar{c}P_L b]\,[\bar{l}P_L \nu_l] + S_R\;[\bar{c}P_R b]\;[\bar{l}P_L \nu_l] + T_L\,[\bar{c}\sigma^{\mu\nu}P_L b]\;[\bar{l}\sigma_{\mu\nu}P_L \nu_l]\Big] \qquad (5.1)\end{aligned}$$

The matix element can be written as:

$$\begin{aligned}M &= \frac{G_F V_{cb}}{\sqrt{2}}\Big[< \lambda_c|[\bar{c}\gamma_\mu(1-\gamma_5)b] + g_V(\bar{c}\gamma_\mu b) + g_A(\bar{c}\gamma_\mu\gamma_5 b)|\lambda_b > [\bar{l}\gamma^\mu(1-\gamma_5)\nu_l] \\ &\quad + < \lambda_c|(g_S\bar{c}b + g_P\bar{c}\gamma_5 b)|\lambda_b > [\bar{l}\gamma^\mu(1-\gamma_5)\nu_l]\Big] \qquad (5.2)\end{aligned}$$

where $g_V = (V_R + V_L)$; $g_A = (V_R - V_L)$; $g_S = (S_R - S_L)$; $g_P = (S_R + S_L)$

The hadronic part of the amplitude is the matrix elements of the weak quark current between

baryonic states that is parametrized in terms of form factors. We defined the six vector and axial vector form factors through the following equations

$$\langle\lambda_c|(\bar{c}\gamma_\mu b)|\lambda_b\rangle = \bar{u}_{\lambda_c}(p_{\lambda_c}, s_{\lambda_c})\Big[f_1\gamma_\mu - 2if_2\sigma_{\mu\nu}q^\nu + f_3 q_\mu\Big]u_{\lambda_b}(p_{\lambda_b}, s_{\lambda_b}), \tag{5.3}$$

$$\langle\lambda_c|(\bar{c}\gamma_\mu\gamma_5 b)|\lambda_b\rangle = \bar{u}_{\lambda_c}(p_{\lambda_c}, s_{\lambda_c})\Big[g_1\gamma_\mu\gamma_5 - 2ig_2\sigma_{\mu\nu}\gamma_5 q^\nu + g_3 q_\mu\gamma_5\Big]u_{\lambda_b}(p_{\lambda_b}, s_{\lambda_b}) \tag{5.4}$$

where $f_1 = {F_1}^V$; $f_2 = (1/M_1){F_2}^V$; $f_3 = (1/M_1){F_3}^V$, and $g_1 = {F_1}^A$; $g_2 = (1/M_1){F_2}^A$; $g_3 = (1/M_1){F_3}^A$, and where $q^\mu = p^\mu - p'^\mu$ is the four momentum transfer.Following Ref. (*Körner and Kramer*, 1992) and Ref. (*Datta*, 1994) we define the helicity amplitudes which are given by

$${H^V}_{\lambda_c,\lambda_w} = {H^V}_{\lambda_{-c},\lambda_{-w}} \tag{5.5}$$

$${H^A}_{\lambda_c,\lambda_w} = -{H^A}_{\lambda_{-c},\lambda_{-w}} \tag{5.6}$$

where λ_c, λ_W are the polarizations of the daughter baryon and the W-boson respectively. In terms of the form factors the helicity amplitudes are given by

$${H^A}_{\lambda_c=1/2,\lambda_w=0} = g_A\frac{\sqrt{Q_+}}{\sqrt{q^2}}\Big((M_1 - M_2)g_1 + q^2 g_2\Big) \tag{5.7}$$

$${H^V}_{\lambda_c=1/2,\lambda_w=0} = g_V\frac{\sqrt{Q_-}}{\sqrt{q^2}}\Big((M_1 - M_2)f_1 - q^2 f_2\Big) \tag{5.8}$$

$${H^V}_{\lambda_c=1/2,\lambda_w=1} = g_V\sqrt{2Q_-}\Big(f_1 - (M_1 + M_2)f_2\Big) \tag{5.9}$$

$${H^A}_{\lambda_c=1/2,\lambda_w=1} = g_A\sqrt{2Q_-}\Big(g_1 + (M_1 - M_2)g_2\Big) \tag{5.10}$$

$$H^{V}{}_{\lambda_c=1/2,\lambda_w=t} = g_V \frac{\sqrt{Q_+}}{\sqrt{q^2}}\Big((M_1 - M_2)f_1 + q^2 f_3\Big) \tag{5.11}$$

$$H^{A}{}_{\lambda_c=1/2,\lambda_w=t} = g_A \frac{\sqrt{Q_-}}{\sqrt{q^2}}\Big((M_1 + M_2)g_1 - q^2 g_3\Big) \tag{5.12}$$

where M_1, M_2 are the parent and daughter baryon masses. The new physics helicity amplitudes are given as

$$H^{S}{}_{\lambda_c=1/2,\lambda_{NP}=0} = g_S \frac{\sqrt{Q_+}}{m_b - m_c}\Big((M_1 - M_2)f_1 + q^2 f_3\Big) \tag{5.13}$$

$$H^{P}{}_{\lambda_c=1/2,\lambda_{NP}=0} = g_P \frac{\sqrt{Q_-}}{m_b + m_c}\Big((M_1 + M_2)g_1 - q^2 g_3\Big) \tag{5.14}$$

$$H^{S}{}_{\lambda_c,\lambda_{NP}} = H^{S}{}_{\lambda_{-c},\lambda_{-NP}} \tag{5.15}$$

$$H^{P}{}_{\lambda_c,\lambda_{NP}} = -H^{P}{}_{\lambda_{-c},\lambda_{-NP}} \tag{5.16}$$

$$H^{SP}{}_{\lambda_c=1/2,\lambda_{NP}=0} \;=\; H^{P}{}_{\lambda_c=1/2,\lambda_{NP}=0} + H^{S}{}_{\lambda_c=1/2,\lambda_{NP}=0} \tag{5.17}$$

The angular distribution following Ref. (*Körner and Kramer*, 1992) and Ref. (*Datta*, 1994) is given as

$$
\begin{aligned}
\frac{d\Gamma(\lambda_b \to \lambda_c \tau^{\mp} \nu_\tau)}{dq^2 d(Cos[\theta_l])} &= \frac{{G_F}^2 {V_{cb}}^2 q^2 |p_{\lambda_c}|}{512\pi^3 {M_1}^2}\left(1-\frac{{m_l}^2}{q^2}\right)^2 \Big[\Big(2Sin[\theta_l](|H_{\lambda_c=1/2,\lambda_w=0}|^2 \\
&+|H_{\lambda_c=-1/2,\lambda_w=0}|^2) + (1-Cos[\theta_l])^2 |H_{\lambda_c=1/2,\lambda_w=1}|^2 \\
&+(1+Cos[\theta_l])^2 |H_{\lambda_c=-1/2,\lambda_w=-1}|^2\Big) + \frac{{m_l}^2}{q^2}\Big(2Cos[\theta_l]^2(|H_{\lambda_c=1/2,\lambda_w=0}|^2 \\
&+|H_{\lambda_c=-1/2,\lambda_w=0}|^2) + Sin[\theta_l]^2(|H_{\lambda_c=1/2,\lambda_w=1}|^2 + |H_{\lambda_c=-1/2,\lambda_w=-1}|^2) \\
&+2(|H_{\lambda_c=1/2,\lambda_w=t}|^2 + |H_{\lambda_c=-1/2,\lambda_w=t}|^2) \\
&-4Cos[\theta_l] Re[(H_{\lambda_c=1/2,\lambda_w=t} cH_{\lambda_c=1/2,\lambda_w=0} \\
&+H_{\lambda_c=-1/2,\lambda_w=t} cH_{\lambda_c=-1/2,\lambda_w=0})]\Big) \\
&+\Big(2(|{H^{SP}}_{\lambda_c=1/2,\lambda_{NP}=0}|^2 + |{H^{SP}}_{\lambda_c=-1/2,\lambda_w=0}|^2) \\
&\frac{4{m_l}^2}{\sqrt{q^2}}(-Cos[\theta_l] Re[(H_{\lambda_c=1/2,\lambda_w=0}\ ({H^{SP}}_{\lambda_c=1/2,\lambda_{NP}=0})^* \\
&+H_{\lambda_c=-1/2,\lambda_w=0}\ ({H^{SP}}_{\lambda_c=-1/2,\lambda_{NP}=0})^*)] \\
&+Re[(H_{\lambda_c=1/2,\lambda_w=t}\ ({H^{SP}}_{\lambda_c=1/2,\lambda_{NP}=t})^* \\
&+H_{\lambda_c=-1/2,\lambda_w=0}\ ({H^{SP}}_{\lambda_c=-1/2,\lambda_{NP}=t})^*)]\Big)\Big] \qquad (5.18)
\end{aligned}
$$

BIBLIOGRAPHY

BIBLIOGRAPHY

A. Esteban-Pretel, J. W. F. V., and P. Huber (2008), Can opera help in constraining neutrino non-standard interactions?, *Phys. Lett. B*, *668*, 197.

A. Friedland, C. L., and C. Pena-Garay (2004), Solar neutrinos as probes of neutrino matter interactions, *Phys. Lett. B*, *594*, 347.

A. M. Gago, H. N. S. U., H. Minakata, and R. Z. Funchal (2010), Resolving cp violation by standard and nonstandard interactions and parameter degeneracy in neutrino oscillations, *JHEP*, *1001*, 049.

A. M. Gago, H. N. W. J. C. T., M. M. Guzzo, and R. Z. Funchal (2001), Probing flavor changing neutrino interactions using neutrino beams from a muon storage ring, *Phys. Rev. D*, *64*, 073,003.

A. Rashed, M. D., and A. Datta (), Nonstandard interactions of atmospheric neutrino via charged higgs and w' contribution, *arXiv:1204.2023 [hep-ph]*.

A.Celis, X.-Q., M.Jung, and A.Pich (), B -¿ d(*) tau nu decays in two-higgs-doublet models, *arXiv:1302.5992 [hep-ph]*.

A.Celis, X.-Q., M.Jung, and A.Pich (2013), Sensitivity to charged scalars in $B \to D^{(*)}\tau\nu_\tau$ and $B \to \tau\nu_\tau$ decays, *JHEP*, *1301*, 054.

A.Crivellin, C., and A.Kokulu (2012), Explaining $b \to d\tau\nu$, $b \to d^*\tau\nu$ and $b \to \tau\nu$ in a 2hdm of type iii, *Phys. Rev. D*, *86*, 054,014.

A.Datta (2006), B(s) mixing and new physics in hadronic b —¿ s anti-q q transitions, *Phys. Rev. D*, *74*, 014,022.

A.Datta, and D.London (2004a), Measuring new physics parameters in b penguin decays, *Phys. Lett. B*, *595*, 453.

A.Datta, and D.London (2004b), Triple-product correlations in b –¿ v1 v2 decays and new physics, *Int. J. Mod. Phys. A*, *19*, 2505.

A.Datta, and M.Duraisamy (2010), Model independent predictions for rare top decays with weak coupling, *Phys. Rev. D*, *81*, 074,008.

A.Datta, and P.J.O'Donnel (2005), The 2-3 symmetry: Flavor changing b, tau decays and neutrino mixing, *Phys. Rev. D*, *72*, 113,002.

A.Datta, D.-V. N., M.Imbeault, and R.Sinha (2005), Methods for measuring new-physics parameters in b decays, *Phys. Rev. D*, *71*, 096,002.

A.Datta, M., and D.Ghosh (2012), Diagnosing new physics in $b \to c\,\tau\,\nu_\tau$ decays in the light of the recent babar result, *Phys. Rev. D*, *86*, 034,027.

A.Datta, M., and D.Ghosh (2014), Explaining the $b \to k^* \mu^+ \mu^-$ data with scalar interactions, *Phys. Rev. D*, *89*, 071,501.

A.Datta, Z.-X., P.J.O'Donnell, and T.Huang (2000), Effects of kaluza-klein excited w on single top quark production at tevatron, *Phys. Lett. B*, *483*, 203.

A.F.Falk, and M.Neubert (1993), Second order power corrections in the heavy quark effective theory. 1. formalism and meson form-factors, *Phys. Rev. D*, *47*, 2965.

A.Friedland, and C.Lunardini (2005), A test of tau neutrino interactions with atmospheric neutrinos and k2k, *Phys. Rev. D*, *72*, 053,009.

A.Friedland, and C.Lunardini (2006), Two modes of searching for new neutrino interactions at minos, *Phys. Rev. D*, *74*, 033,012.

A.K.Alok, A.-M. D., A.Datta, and D.London (2011), New physics in $b- > s\mu^+\mu^-$: Cp-conserving observables, *JHEP*, *1111*, 122.

Alsharoa, M. M., et al. (2003), Recent progress in neutrino factory and muon collider research within the Muon collaboration, *Phys.Rev.ST Accel.Beams*, *6*, 081,001.

A.Rashed, M., and A.Datta (2012), Corrections to the atmospheric neutrino mixing from charged higgs and w' contribution to ν_τ-nucleon scattering, *arXiv:1204.2023*.

A.Rashed, P., and A.Datta (2013), Tau neutrino as a probe of nonstandard interaction, *Nucl. Phys. B*, *877*, 662.

C. Biggio, M. B., and E. Fernandez-Martinez (2009), General bounds on non-standard neutrino interactions, *JHEP*, *0908*, 090.

C.-W.Chiang, M. D. M., A.Datta, and A.Szynkman (2010), New physics in b0(s) —¿ j/psi phi: A general analysis, *JHEP*, *1004*, 031.

Campanelli, M., and A. Romanino (2002), Effects of new physics in neutrino oscillations in matter, *Phys. Rev. D*, *66*, 113,001.

Datta, A. (1994), Semi-leptonic decays of $\mathbf{\Lambda_c}$ and $\mathbf{\Lambda_b}$ baryons involving heavy to light transitions and the determination of $|\mathbf{v_{ub}}|$, *arXiv:hep-ph/9504429*.

D.Becirevic, N., and A.Tayduganov (2012), $\bar{b} \to d\tau\bar{\nu}_\tau$ vs. $\bar{b} \to d\mu\bar{\nu}_\mu$, *Phys. Lett. B*, *716*, 208.

D.Choudhury, D., and A.Kundu (2012), B decay anomalies in an effective theory, *Phys. Rev. D*, *86*, 114,037.

DELPHI (2005), Photon events with missing energy in e+ e- collisions at s**(1/2) = 395.

Diaz, R. A. (), Phenomenological analysis of the two higgs doublet model, *hep-ph/0212237*.

D.V.Forero, M., and J.W.F.Valle (), Global status of neutrino oscillation parameters after neutrino-2012, *arXiv:1205.4018 [hep-ph]*.

E. A. Paschos, L. P., and J. Y. Yu (2000), *Nucl. Phys. B*, *588*, 263.

et al. (DONuT Collaboration), K. K. (2008), Final tau-neutrino results from the donut experiment, *Phys. Rev. D*, *78*, 052,002.

et al. (OPERA Collaborarion), N. A. (2010), Observation of a first nu_τ candidate in the opera experiment in the cngs beam, *Phys.Lett. B*, *691*, 138.

et al. (BABAR Collaboration), J. P. L. (2012), Evidence for an excess of $\bar{B} \to d^{(*)}\tau^-\nu_\tau$ decays, *Phys. Rev. Lett.*, *109*, 101,802.

F. J. Escrihuela, M. A. T., O. G. Miranda, and J. W. F. Valle (2009), Constraining nonstandard neutrino-quark interactions with solar, reactor and accelerator data, *Phys. Rev. D*, *80*, 105,009.

Gonzalez-Garcia, M. C., and M. Maltoni (2004), Atmospheric neutrino oscillations and new physics, *Phys. Rev. D*, *70*, 033,010.

H.E.Haber (1994), Spin formalism and applications to new physics searches, *[hep-ph/9405376]*, pp. 231–272.

HFAG (2010), Averages of b-hadron, c-hadron, and τ lepton properties, *arXiv:1010.1589 [hep-ex]*.

Huber, P., and J. W. F. Valle (2001), Nonstandard interactions: Atmospheric versus neutrino factory experiments, *Phys. Lett. B*, *523*, 151.

I.Caprini, L., and M.Neubert (1998), Dispersive bounds on the shape of $\bar{B} \to d^* l \bar{\nu}_l$ form-factors, *Nucl. Phys. B*, *530*, 153.

I.Dorner, N., S.Fajfer, and I.Niandi (2013), Minimally flavored colored scalar in $\bar{b} \to d^{(*)}\tau\bar{\nu}$ and the mass matrices constraints, *JHEP*, *1311*, 084.

I.I.Bigi, and A.I.Sanda (2005), A 'known' cp asymmetry in tau decays, *Phys. Lett. B*, *625*, 47.

J. Barranco, O. G. M., and T. I. Rashba (2005), Probing new physics with coherent neutrino scattering off nuclei, *JHEP*, *0512*, 021.

J. Barranco, O. G. M., and T. I. Rashba (2007), Low energy neutrino experiments sensitivity to physics beyond the standard model, *Phys. Rev. D*, *76*, 073,008.

J. Kopp, M. L., and T. Ota (2007), Discovery reach for non-standard interactions in a neutrino factory, *Phys. Rev. D*, *76*, 013,001.

J. Kopp, T. O., and W. Winter (2008), Neutrino factory optimization for non-standard interactions, *Phys. Rev. D*, *78*, 053,007.

J. Kopp, T. O., M. Lindner, and J. Sato (2008), Non-standard neutrino interactions in reactor and superbeam experiments, *Phys. Rev. D*, *77*, 013,007.

J.G.Korner, and G.A.Schuler (1989), Lepton mass effects in semileptonic b meson decays, *Phys. Lett. B*, *231*, 306.

J.G.Korner, and G.A.Schuler (1990), Exclusive semileptonic heavy meson decays including lepton mass effects, *Z. Phys. C*, *46*, 93.

J.M.Arnold, B., and M.B.Wise (2013), Phenomenology of scalar leptoquarks, *Phys. Rev. D*, *88*, 035,009.

K. Hagiwara, K. M., and H. Yokoya (2003), Tau polarization in tau neutrino nucleon scattering, *Nucl. Phys. B*, *668*, 364.

K.Hagiwara, M., and Y.Sakaki (), Cp violation in $b \to d\tau\nu_\tau$ using multi-pion tau decays, *arXiv:1403.5892 [hep-ph]*.

Kodama, K., et al. (2001), Observation of tau neutrino interactions, *Phys.Lett.*, *B504*, 218–224, doi:10.1016/S0370-2693(01)00307-0.

Körner, J., and M. Kramer (1992), *Phys. Lett.*, *275*, 495.

M. Blennow, T. O., and W. Winter (2007), Non-standard hamiltonian effects on neutrino oscillations, *Eur. Phys. J. C*, *49*, 1023.

M. C. Gonzalez-Garcia, A. G., Y. Grossman, and Y. Nir (2001), New cp violation in neutrino oscillations, *Phys. Rev. D*, *64*, 096,006.

M. Malinsky, T. O., and H. Zhang (2009), Non-standard neutrino interactions from a triplet seesaw model, *Phys. Rev. D*, *79*, 011,301.

M.Beneke, and T.Feldmann (2001), Symmetry breaking corrections to heavy to light b meson form-factors at large recoil, *Nucl. Phys. B*, *592*, 3.

M.Blennow, T., and J.Skrotzki (2008), Effects of non-standard interactions in the minos experiment, *Phys. Lett. B*, *660*, 522.

M.C.Gonzalez-Garcia, M., and J.Salvado (2010), Updated global fit to three neutrino mixing: status of the hints of theta13 ¿ 0, *JHEP*, *1004*, 056.

M.C.Gonzalez-Garcia, P. H. O. V. J., M.M.Guzzo, and R. Funchal (1999), Msw effect with flavor changing neutrino interactions, *Phys. Rev. Lett.*, *82*, 3202.

M.Duraisamy, and A.Datta (2013), The full $b \to d^*\tau^-\bar{\nu_\tau}$ angular distribution and cp violating triple products, *JHEP*, *1309*, 059.

M.Duraisamy, A., and A.Datta (2011), The top forward backward asymmetry with general z' couplings, *Phys. Rev. D*, *84*, 054,018.

M.Guzzo, M. H. M., P.C.de Holanda, and J.W.F.Valle (2002), Status of a hybrid three neutrino interpretation of neutrino data, *Nucl. Phys. B*, *629*, 479.

M.Honda, K., T.Kajita, and S.Midorikawa (2011), Improvement of low energy atmospheric neutrino flux calculation using the jam nuclear interaction model, *Phys. Rev. D*, *83*, 123,001.

Mikheyev, S., and A. Smirnov (1985), *Sov. J. Nucl. Phys.*, *42*, 913.

M.M.Guzzo, A., and S.T.Petcov (1991), On the msw effect with massless neutrinos and no mixing in the vacuum, *Phys. Lett*, *154*, 154.

M.M.Guzzo, P. H., H.Nunokawa, and O.L.G.Peres (2001), On the massless 'just-so' solution to the solar neutrino problem, *Phys. Rev. D*, *44*, 097,301.

M.Tanaka, and R.Watanabe (), New physics in the weak interaction of $\bar{b} \to d^{(*)}\tau\bar{\nu}$, *arXiv:1212.1878 [hep-ph]*.

N. C. Ribeiro, H. N. S. U., H. Minakata, and R. Zukanovich-Funchal (2007), Probing non-standard neutrino interactions with neutrino factories, *JHEP*, *0712*, 002.

N. C. Ribeiro, T. K. S. N. P. K., H. Nunokawa, and H. Minakata (2008), Probing nonstandard neutrino physics by two identical detectors with different baselines, *Phys. Rev. D*, *77*, 073,007.

N. Fornengo, R. T., M. Maltoni, and J. W. F. Valle (2002), Probing neutrino nonstandard interactions with atmospheric neutrino data, *Phys. Rev. D*, *65*, 013,010.

Neuffer, D. (1981), Design of Muon Storage Rings for Neutrino Oscillations Experiments. (Talk), *IEEE Trans.Nucl.Sci.*, *28*, 2034–2036.

N.G.Deshpande, and A.Menon (), Hints of r-parity violation in b decays into $\tau\nu$, *arXiv:1208.4134 [hep-ph]*.

N.Kitazawa, H., and O.Yasuda (2006), Will minos see new physics, *hep-ph/0606013*.

O. G. Miranda, M. A. T., and J. W. F. Valle (2006), Are solar neutrino oscillations robust?, *JHEP*, *0610*, 008.

P. Coloma, J. L.-P., A. Donini, and H. Minakata (2011), Non-standard interactions at a neutrino factory: Correlations and cp violation, *JHEP*, *1108*, 036.

Palazzo, A., and J. W. F. Valle (2009), Confusing non-zero theta(13) with non-standard interactions in the solar neutrino sector, *Phys. Rev. D*, *80*, 091,301.

Paschos, E. A., and J. Y. Yu (2002), *Phys. Rev. D*, *65*, 033,002.

P.Biancofiore, P., and F. Fazio (), On the anomalous enhancement observed in $b \to d^{(*)}\,\tau\,\bar{\nu}_\tau$ decays, *arXiv:1302.1042 [hep-ph]*.

PDG (2010), Review of particle physics, *J. Phys. G G*, *37*, 075,021.

R. Adhikari, A. D., S. Chakraborty, and S. Roy (2012), Non-standard interaction in neutrino oscillations and recent daya bay, t2k experiments, *Phys. Rev. D*, *86*, 073,010.

S. Bergmann, Y. G., and D. M. Pierce (2000), Can lepton flavor violating interactions explain the atmospheric neutrino problem?, *Phys. Rev. D*, *61*, 053,005.

S. Davidson, N. R., C. Pena-Garay, and A. Santamaria (2003), Present and future bounds on non-standard neutrino interactions, *JHEP*, *0303*, 011.

S. K. Agarwalla, F. L., and T. Takeuchi (2012), Constraining non-standard interactions of the neutrino with borexino, *JHEP*, *1212*, 079.

S.Baek, P. O., A.Datta, and D.London (2005), Polarization states in b —¿ rho k* and new physics, *Phys. Rev. D*, *72*, 094,008.

S.Bergmann, P. H. P., M.M.Guzzo, and H.Nunokaw (2000), Status of the solution to the solar neutrino problem based on nonstandard neutrino interactions, *Phys. Rev. D*, *62*, 073,001.

S.Fajfer, J., and I.Nisandzic (), *arXiv:1203.2654 [hep-ph]*.

Super-Kamiokande (2011), Study of non-standard neutrino interactions with atmospheric neutrino data in super-kamiokande i and ii, *Phys. Rev. D*, *84*, 113,008.

Super-Kamiokande (2012), A measurement of the appearance of atmospheric tau neutrinos by super-kamiokande, *arXiv:1206.0328 [hep-ex]*.

T. Ohlsson, H. Z., and S. Zhou (2013), Effects of nonstandard neutrino interactions at pingu, *Phys. Rev. D*, *88*, 013,001.

T. Ota, J. S., and N. a. Yamashita (2002), Oscillation enhanced search for new interaction with neutrinos, *Phys. Rev. D*, *65*, 093,015.

T.Ota, and J.Sato (2002), Can icarus and opera give information on a new physics, *Phys. Lett. B*, *545*, 367.

W.Bensalem, A., and D.London (2002a), New physics effects on triple product correlations in lambda(b) decays, *Phys. Rev. D*, *66*, 094,004.

W.Bensalem, A., and D.London (2002b), T violating triple product correlations in charmless lambda(b) decays, *Phys. Lett. B*, *538*, 309.

W.Buchmuller, R., and D.Wyler (1987), Leptoquarks in lepton - quark collisions, *Phys. Lett. B*, *191*, 442.

Wolfenstein, L. (1978), *Phys. Rev.D*, *17*, 2369.

Y.-Y.Fan, W.-F., and Z.-J.Xiao (), Semileptonic decays $b \to d^{(*)} l\nu$ in the perturbative qcd factorization approach, *arXiv:1301.6246 [hep-ph]*.

Y.Grossman (1995), Nonstandard neutrino interactions and neutrino oscillation experiments, *Phys. Lett. B*, *395*, 141.

Y.Grossman, and Y.Nir (2002), *JHEP*, *1204*, 002.

Y.Sakaki, and H.Tanaka (), Constraints of the charged scalar effects using the forward-backward asymmetry on $b \to d^{(*)}\tau\bar{\nu_\tau}$, *arXiv:1205.4908 [hep-ph]*.

Y.Sakaki, A., M.Tanaka, and R.Watanabe (2013), Testing leptoquark models in $\bar{b} \to d^{(*)}\tau\bar{\nu}$, *Phys. Rev. D*, *88*, 094,012.

Z. Berezhiani, R. S. R., and A. Rossi (2002), Probing nonstandard couplings of neutrinos at the borexino detector, *Nucl. Phys. B*, *638*, 62.

VITA

Preet Sharma

phone: (254)716-9347
preetsharma242805@gmail.com
psharma@go.olemiss.edu

EDUCATION

PhD Dec. 2014
University of Mississippi
Department of Physics and Astronomy
Dissertation: "Probing New Physics with Third Generation Lepton"
Committee: Dr. Alakabha Datta (Chair), Dr. Don Summers,
Dr. Lucien Cremaldi, Dr. Luca Bombelli,
Dr. Micah B. Milinovich

Graduate Student Aug. 2006 - Aug. 2009
Baylor University
Department of Physics
Research Advisor: Dr. Anzhong Wang

MS Sep. 2004
Indian Institute of Technology, Roorkee(IIT Roorkee), India
Department of Physics
Thesis: "Study of High Altitude Lightning"
Thesis Advisor: Dr. Jagdish Rai

BS(Honors) Jul. 2002
Ranchi University, India
Department of Physics
Physics(Honors)

HONORS & AWARDS

Physics Department Honors Award 2009, 2010, 2011

Department of Physics and Astronomy
University of Mississippi

Physics Honors Award 1998, 1999, 2000, 2001
Department of Physics
Ranchi University, India

TEACHING EXPERIENCE

University of Mississippi Aug. 2009 - Jul. 2014
Department of Physics and Astronomy
Graduate Teaching Assistant

- Taught Astronomy 103 and 104 labs to around 100 undergraduates every semester which required 30-40 minutes of lecturing and then monitoring and supervising indoor and outdoor labs.
- Received excellent student evaluations.
- Developed and graded labs reports and revised lab syllabus.
- Volunteered towards the construction of outdoor site for astronomy teaching called ”Dark Site”.
- Coordinated outdoor trips to ”Dark Site” astronomy sessions.
- Coordinated labs with other teaching assistants.
- Volunteered for tutorial sessions for physics and astronomy.

Baylor University Aug. 2006 - Jul. 2009
Department of Physics
Graduate Teaching Assistant

- Taught physics labs to around 45 undergraduates every semester which required 20-30 minutes of lecturing and then monitoring and supervising them.
- Received excellent student evaluations.
- Developed and graded labs reports and revised lab syllabus.
- Volunteered for tutorial sessions for physics.
- Coordinated with other teaching assistants in development and revision of lab syllabus and teaching duties.

Dr. B.R. Ambedkar Inter College, India Jul. 2004 - Jun. 2005
Department of Science
Lecturer of Physics and Mathematics

- Taught physics and mathematics to around 30 students every semester, which required 1 hr of lecturing and 1 hr of problem solving sessions.
- Prepared the curriculum and lectures.
- Coordinated tutorial sessions.

Dr. B.R. Ambedkar Inter College, India Mar. 2000 - May 2002
Department of Science
Lecturer of Physics and Mathematics

- Taught physics and mathematics to around 30 students every semester, which required 1 hr of lecturing and 1 hr of problem solving sessions.
- Prepared the curriculum and lectures.
- Coordinated tutorial sessions.

PUBLICATIONS

- Duraisamy, Murugeswaran , Sharma, Preet , Datta, Alakabha, "The Azimuthal $B \to D^* \tau^- \bar{\nu_\tau}$ Angular Distribution with Tensor Operators", Physicsl Review D90 (2014) 7, 074013.
- Rashed, Ahmed , Sharma, Preet , Datta, Alakabha, "Tau neutrino as a probe of nonstandard interaction", Nuclear Physics B 877 (2013) 662-682.
- Sharma, Preet , Tziolas, Andreas , Wang, Anzhong , Wu, Zhong Chao, "Spacetime Singularities in String and its Low Dimensional Effective Theory", International Journal of Modern Physics A26 (2011), 273-300.

RESEARCH TRAVEL GRANTS

- Graduate research award to present my research at Mississippi Academy of Sciences (MAS), 78th Annual Meeting, 06 March 2014, Hattiesburg MS.
- Graduate research award to present my research at Phenomenology 2013 Symposium, 06 May-08 May 2013, Pittsburgh PA.
- Graduate research award for Phenomenology 2013 Symposium, 76 May-09 May 2012, Pittsburgh PA.
- Graduate award for "Gravity Meeting", October 2009, University of Michigan, Ann Arbor MI.

- Travel award to attend "Workshop on Cosmology and Strings", 09 July-13 July 2007, Abdus Salam International Centre for Theoretical Phycics, Miramare-Trieste, Italy.
- Graduate travel award to present my research "Cosmology of Orbifold Branes in Superstring", American Physical Society's Fall Meeting, 19 October 2007, Texas A&M University, College Station TX.
- Graduate travel award to attend the conference and workshop "Origins of Dark Energy", 14 May-17 May 2007, McMaster University, Hamilton Canada.

CONFERENCE PRESENTATIONS

- "Tau neutrino as a probe of nonstandard interaction", Mississippi Academy of Sciences (MAS), 78th Annual Meeting, 06 March 2014, Hattiesburg MS.
- "Neutrino Nucleon Scattering", Phenomenology 2013 Symposium, 06 May-08 May 2013, Pittsburgh PA.
- "A Review of Dark Matter", Department of Physics and Astronomy, University of Mississippi, 28 September 2010, Oxford MS
- "Cosmology of Orbifold Branes in Superstring", American Physical Society's Fall Meeting, 19 October 2007, Texas A&M University, College Station TX.

CONFERENCES & WORKSHOPS

- "Mississippi Academy of Sciences (MAS)", 78th Annual Meeting, 06 March 2014, Hattiesburg MS.
- "Phenomenology 2013 Symposium", 06 May-08 May 2013, Pittsburgh PA.
- "Phenomenology 2013 Symposium", 76 May-09 May 2012, Pittsburgh PA.
- "Gravity Meeting", October 2009, University of Michigan, Ann Arbor MI.
- "American Physical Society's Fall Meeting", 19 October 2007, Texas A&M University, College Station TX.
- "Workshop on Cosmology and Strings", 09 July-13 July 2007, Abdus Salam International Centre for Theoretical Phycics, Miramare-Trieste, Italy.
- "Origins of Dark Energy", 14 May-17 May 2007, McMaster University, Hamilton Canada.

COMMUNITY SERVICE

University of Mississippi

- Open house astronomy sessions held every month at the Department of Physics and Astronomy, Aug. 2009 - Jul. 2014.
- Volunteered towards the construction of the outdoor site for astronomy teaching called "Dark Site".
- Free physics tutoring for financially poor students, Aug. 2009 - Jul. 2014.
- Science fair judge held at the University of Mississippi.

COMPUTER SKILLS

Languages & Software: Python, R, Rapidminer, Tableau, Java, Mathematica, Fortran, Hadoop, MySql, Pig, Hive, Sqoop, ZooKeeper, HBase, MongoDB, Shell Scripting.

Operating Systems: Linux, Windows.

Certifications:

- The Data Scientists Toolbox: Offered by John Hopkins University
- Big Data Fundamentals: Big Data University.
- Introduction to Pig: Big Data University.
- Introduction to MapReduce Programming: Big Data University.
- Moving Data into Hadoop: Big Data University.
- Hadoop Fundamentals: Big Data University.
- Introduction to Data Analysis using R: Big Data University.

REFERENCES

- **Dr. Alakabha Datta**
  Office: 209 Lewis Hall
  Department of Physics and Astronomy
  University of Mississippi
  Phone: (662)915-5611
  Email: datta@phy.olemiss.edu
- **Dr. Luca Bombelli**
  Office: 211B Lewis Hall
  Department of Physics and Astronomy
  University of Mississippi

Phone: (662)915-5319
Email: luca@phy.olemiss.edu

- **Dr. Murugeswaran Duraisamy**
  Office: 225 Lewis Hall
  Department of Physics and Astronomy
  University of Mississippi
  Phone: (662)915-5965
  Email: duraism@phy.olemiss.edu, mduraisa@gmail.com

- **Mr. James Hill**
  Office: Kennon Observatory Room 1
  Department of Physics and Astronomy
  University of Mississippi
  Phone: (662)915-7928
  Email: jhill6333@gmail.com
